Nonclassical Block Copolymer Self-Assembly Resulting from a Constrained Location of Chains and Junctions

Yushu Matsushita, Atsushi Takano, Marylène Vayer, Christophe Sinturel

Non-classical block-copolymer self-assembly resulting from a constrained location of chains and junctions

Yushu MATSUSHITA,[1] Atsushi TAKANO,[1] Marylène VAYER,[2] Christophe SINTUREL[2]

[1] Department of Molecular & Macromolecular Chemistry, Grad. School of Engineering, Nagoya University, Furo-cho, Chikusa-ku, Nagoya 464-8603, Japan

[2]Interfaces, Confinement, Matériaux et Nanostructures (ICMN) UMR 7374, CNRS-Université d'Orléans, CS 40059, F-45071 Orléans, France

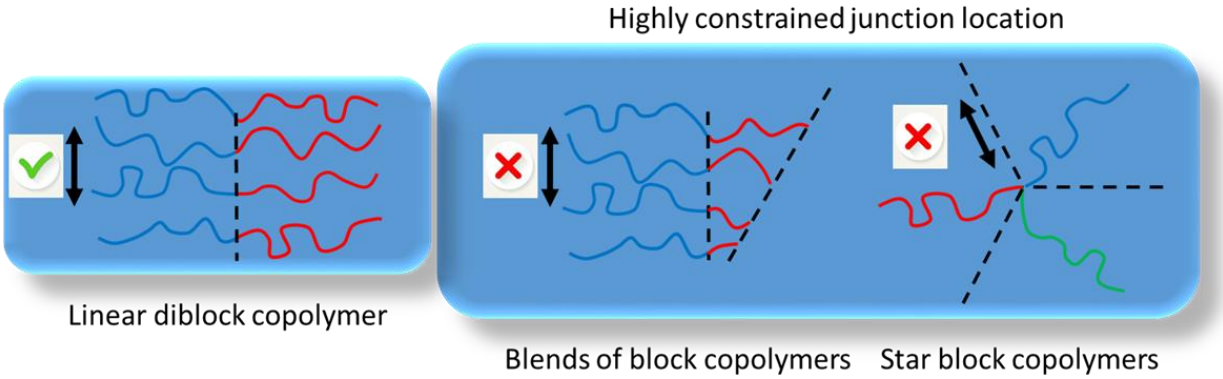

Abstract

During the self-assembly process of block-copolymers, interfaces are formed as a result of the microphase separation between the blocks. The location of the polymer chains and block junctions with respect to these interfaces is crucial and drives the morphology. It depends on the dispersities (e.g. molecular mass and composition) of the blocks, their architectures (e.g. linear vs star) and the type of interaction (e.g. repulsion vs attraction). In this review, we focus on the formation of unusual morphologies that have been obtained in the following three categories: i) multimodal blends of block polymers, ii) star block polymers and iii) supramolecular assemblies composed of block copolymers. Although these three examples seem to be very different from one another, we will demonstrate in this review that they all share a constrained location of their chains and/or junctions with respect to the interfaces. In this sense, they deviate from the common behavior of simple linear block copolymers, in which the junctions are located on the interface and homogeneously distributed onto it.

Introduction

Block copolymers are renowned for their ability to self-assemble into a rich variety of ordered phases, producing intriguing morphologies on the scale of the natural dimension of the macromolecules (i.e. from a few to some tens of nm). Composed of chemically distinct blocks, such compounds spontaneously undergo microphase separation in the melt when repulsion of the blocks dominates. This is simply a direct consequence of the natural tendency of dissimilar polymers to phase separate, but because of the covalent bonds that connect the blocks, the phase separation is restricted to the scale of the polymer chains' dimension. During the self-assembly process, new interfaces are formed as a result of the microphase separation between the blocks. The location of the polymer chains and block junctions with respect to these interfaces is crucial and depends on the architecture of the block copolymers (e.g. linear vs star) and/or on the type of interaction (e.g. repulsion vs attraction).

In the case of simple linear block copolymers, the block junctions are located on the interfaces.[1]At both sides of the interface, the polymer block chains tend to stretch (resulting in an entropic penalty) because of the repulsion at the interface under the condition of filling space uniformly. The balance between interfacial tension and chain stretching determines the equilibrium size of the microdomains and dictates the geometry of the structure.[2] In this case, none of the chains have a selected location: any individual chain in the system is virtually interchangeable with another one, without compromising the integrity of the morphology (it just needs to accommodate its amount of stretching). The situation is rather different in systems with a multimodal dispersity (i.e. blocks having a marked discontinuous variation in length), that can be obtained by blending blocks with the same chemical composition but with different lengths and narrow dispersities. In this case, the location of the chains around the interface can be heterogeneous, creating new morphologies that do not exist in classical phase diagrams.

In star-shaped polymers, blocks share a single common junction. In the simplest ABC star-shaped terpolymer, a three-phase structure is formed with all the junctions located at the boundary of the A/B/C micro-domains, i.e., no junctions can be found at the A/C, A/B or B/C boundaries as is the case in linear copolymers. For example, for an A/B/C 1:1:1 arm length ratio, this very restricted alignment of their junction points along a single line produces a unique set of anisotropic cylinder-based structures, whose cross section adopts a two-dimensional tiling pattern with polygonal domains (i.e. flat interfaces and sharp corners).[3]

Lastly, if specific intermolecular interactions (such as hydrogen bonding) are introduced into a block copolymer blend, hierarchical self-assembled patterns can be formed. Again, the location of chains and junctions follows very specific rules compared to simple block copolymer systems. The miscibility of blocks can lead to a complex single phase. For example, the blend of two incompatible block polymers AB and CD leads to macrophase separation whereas if B and C are interactive via hydrogen bonding, several hierarchical structures can be formed depending on the composition and volume ratio.[4]

In all these three cases (multimodal blends of copolymers, star-shaped block copolymers and supramolecular assemblies), the self-assembled morphology differs from the simple linear block copolymer case which constitutes the common behavior, with junctions located on the interface of the domains and homogeneously distributed onto it. In this review, we re-examine the formation of unusual morphologies through the angle of the location of the polymer chains and block junctions with respect to the interfaces. We will demonstrate how they differ from the simple linear block copolymer case. The first part of this report will detail morphologies obtained in blends of block polymers having different chain lengths. In the second part, we will describe the behavior of star-shaped polymers producing Archimedean type tiling patterns and even more complex tilings including quasicrystalline tilings. The last

part will be devoted to block copolymer blends which are forced to mix by hydrogen-bonding interaction.

Part1: From monomodal to multimodal dispersity using blends of block copolymers

Introduction

During microphase separation, the balance between interfacial tension and stretching of polymer chains determines the equilibrium size of the microdomains and dictates the geometry of the structure. For example, planar interfaces are formed in the case of symmetric linear polymers, but as soon as the polymer becomes asymmetric, phase transition occurs as a result of the interface curvature that balances the degree of stretching of the blocks. Even in the simplest case of AB diblock copolymers, a rich set of morphologies has been described, ranging from symmetric to highly asymmetric copolymers: lamellae (L), perforated lamellae (PL), gyroid (G), cylinder (C) and spheres (S). Up to a reasonable level of unimodal dispersity (i.e. a continuous distribution of molar mass and block composition around a single maximum value), block polymers exhibit similar phase diagrams. As soon as the dispersity increases more significantly, phase behavior can be affected, with a tendency to curve the interface toward the domains having chains with wide dispersity.[5],[6] This result arises from the large variety in chain lengths, reducing the entropic penalty associated with filling the center of the domains in comparison to a monodisperse system. However, the morphologies observed in such cases remain "classical" such as L, G, C or S and only the phase diagram boundaries are modified. To go beyond this and trigger new behaviors in the self-assembly of block copolymers, a substantial amount of work arising from blends of block copolymers having the same chemistry (i.e. the same blocks), but differing in average molar mass and/or composition has been reported. Each of the single components possesses a narrow distribution in chain

length and composition, while the resulting blend can be considered multimodal.[7] As long as the copolymers remain miscible at the molecular level, the junctions of the blocks share the same interfaces. The examination of the literature shows that such systems fall into two categories.

In the first one, the binary mixtures behave like pure polymers and the morphology is controlled by the volume fraction of each block. For example, Koneripalli et al.[8] studied the blending of two asymmetric polystyrene-b-poly(2-vinylpyridine) (PS-*b*-P2VP) block copolymers with the same molar mass but different volume fractions of PS, and showed that the blend with a PS volume fraction of 0.5 leads to a lamellar structure.

In the second one, strong modification of the phase boundaries can occur. In this case, the work of Court et al.[9] on the key concept of "cosurfactant-effect" is particularly relevant. This effect has mostly been demonstrated in a landmark series of studies dealing with the morphological behavior of binary mixtures of polystyrene-*b*-polyisoprene diblock copolymers (PS-*b*-PI) composed of a long asymmetric and a short symmetric copolymer. In that work, it was proved that the chain length ratio drives the curvature of the interface, breaking the usual relationship between morphology and volume fraction. Although severe distortion of the phase diagram picture was highlighted in the work, no new morphology was encountered in the range of composition and chain length ratio studied. By adopting the same kind of concept, but using block copolymers exhibiting a larger dispersity in their molar mass and/or more complex architectures (triblock terpolymers instead of simple diblocks), new morphologies differing from the classical morphology have been reported. Below is our view of the most striking results reported so far in the literature.

Blends of diblocks

In a very recent paper of 2019, Takagi et al.[10] succeeded in stabilizing a double diamond network from ternary blends of diblocks, although it is difficult to form this structure in

classical diblock phase diagrams. This kind of morphology is indeed known to be unstable due to its high interfacial area and large variation in the domain thickness, which imposes a wide distribution in the amount of chain-stretching. In their work, the authors used ternary blends of diblocks (polystyrene-*b*-polyisoprene) (PS-*b*-PI) with almost the same PS molar mass (c.a. 100 kg.mol^{-1}) but different molar masses of PI (96, 52 and 31 kg.mol^{-1}) exhibiting lamellar, gyroid and cylindrical structures, respectively. Among all the blends studied in this work, specific proportions in the ternary blend led to double diamond (DD) structures with a matrix of PS and double four-branched networks of PI, as demonstrated by TEM and SAXS analyses. These results are in contrast with earlier work by this group with blends of polystyrene-*b*–poly(2-vinylpyridine) (PS-*b*-P2VP) diblocks where the lamellar structure was preserved[11] (even in the case of blending 9 different PS-*b*-P2VP diblock copolymers that have a fraction of PS ranging from 0.1 to 0.9). In the work by Takagi et al., the demixing of three chains with different PI lengths allows for stabilizing the diamond structure although the interfacial area is increased. The chains adopt selected locations along the interface, which leads to a loss of translational entropy, but the system gains in conformational entropy and releases packing frustration. The long chains of PI selectively fill the thicker connections (nodes), short chains fill the channels and the medium chains smooth the system (Figure 1.1). As stressed by the authors, the three chains play individual roles to save conformational entropy, resulting in forming the DD structures.

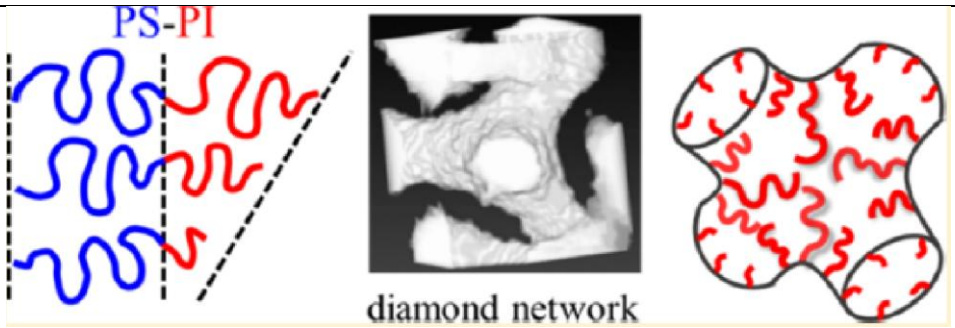

Figure 1.1: A TEM tomography image and the corresponding schematic representation for PI network showing the location of the three PI chains in PS-*b*-PI block polymers in Takagi et al.[10]. Reprinted with permission from ref 10. Copyright (2019) American Chemical

This special spatial placement of the block copolymers is described by the authors as a "weak" localization, as blocks of different sizes can mix at the mesoscopic scale (in opposition to a "strong" localization where all the blocks of a given size segregate in given domains). It is worth noting that mixing block polymers with strong compositional heterogeneity does not always lead to such a "weak" localization. Chen et al. in a 2006 paper [12] showed that mixing two polystyrene-*b*-polymethylmetacrylate (PS-*b*-PMMA) block copolymers having the same molar mass (c.a. 200 $kg.mol^{-1}$) but a large difference in composition (PS volume fractions of 0.3 and 0.7) actually leads to a multilayered microphase structure, with a partition of the different types of block polymers along different interfaces. The resulting morphology consists in a PS core and multiple shells of PMMA, PS and PMMA (see Figure S1-1 in supplementary information). In this case, a localization of the different junction points along a single interface ("weak" localization) would induce a too severe packing frustration. Instead, the authors proposed that the two block copolymers' junctions are located on separate interfaces. The PS are located in separate domains (core for a given population and shell for another one) that can be described as a "strong" localization. The PMMA adopt a bilayer morphology in a common domain that can be described as a "weak" localization. In this case, the thin film configuration as well as the use of selective solvent account for this specific behavior. A similar effect was reported in thin films of blends of two asymmetric polystyrene-*b*-polybutadiene (PS-*b*-PB) studied by Guo and coworkers[13]. As an example, two PS-*b*-PB with total molar masses of 137 and 96.5 $kg.mol^{-1}$, volume fractions of PS equal to 0.24 and 0.62 and polydispersities smaller than 1.1 were considered. With these volume fractions, the two parent polymers exhibited a cylindrical structure, with PS cylinders in a PB matrix for the first one and PB cylinders in a PS matrix for the second one. Exposing thin films of these polymer blends with a 0.5:0.5 weight ratio to cyclohexane, a good solvent

of PB and a theta solvent of PS, led to an original structure named by the authors "sphere between cylinders" and presented in Figure S1-2. This configuration is described as a matrix of PB (blending of the blocks of the two copolymers) and two phases of PS (one for each copolymer) and is attributed to the large viscosity of the system and the slow rearrangement kinetic. In this case, the PB chains encounter weak localization while the PS chains encounter strong localization.

Blends of triblocks

The situation with blends containing triblocks is different from their diblock counterparts since they possess a central block that imposes a bridge type conformation. This specific feature is responsible for a larger variety of very specific behaviors that we will now detail.

The first example deals with a blend of three symmetric polyisoprene-*b*-styrene-*b*-2-vinylpridine) ((PI-*b*-PS-*b*-P2VP) named ISP) block copolymers (volume fractions of PI, PS, P2VP equal to 0.33 for all three ISP) having different molar masses (2.6, 9.6 and 15 $kg.mol^{-1}$). The three parent polymers all show a three-phase lamellar structure (four layers PI-PS-PVP-PI), with a lattice spacing increasing with the molar mass. Each polymer was prepared using a three-step anionic polymerization, and hence the dispersity of each block is low (ranging from 1.03 to 1.04). By blending the three polymers in various proportions in a common solvent (THF), bulk samples with various block dispersities (ranging from 1.1 to 1.5) were obtained after slow evaporation and thermal annealing. The blends having lower dispersity exhibited a classical lamellar structure, whereas an undulated lamellar structure was obtained for higher values[14] (Figure 1.2). Compared to the diblock case described above, the presence of the PS middle-block in ISP terpolymers imposes a bridge conformation, leading to a particular placement of the chains as depicted in Figure 1.2. The new structure was attributed to the selected and periodic localization of junction points of the three parent polymers. The short

chains fill the narrow spaces, the long chains are located in the wider spaces and the middle ones are in the intermediate location. This spatial placement of the block copolymers ("weak" localization) allows the repetition of the block junctions in a periodic fashion along the interfaces. In such a structure, the loss in translational entropy arising from the weak localization of junction points was considered to be counterbalanced by the gain in conformational entropy compared to a lamellar structure with a flat surface. However, this was not confirmed by theoretical calculation.

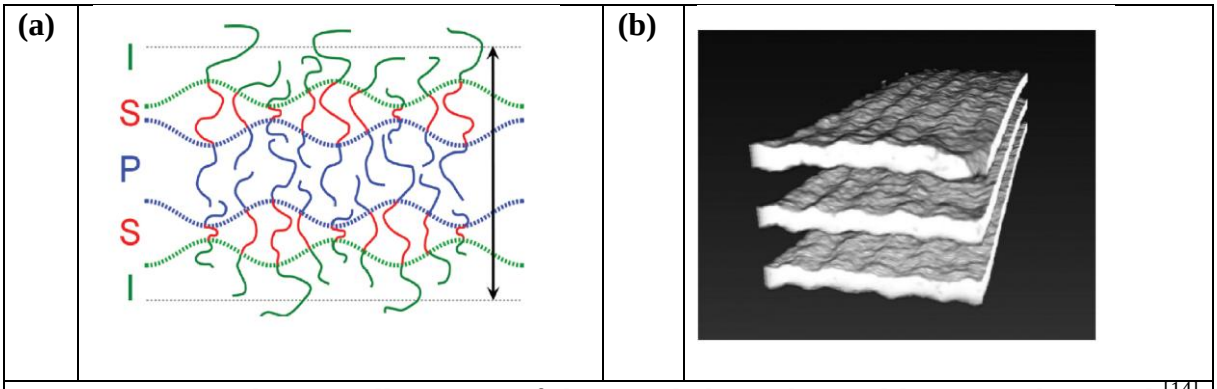

Figure 1.2: (a) Schematic illustration of the morphology observed by Matsushita et al.[14] for a blend of three symmetric PI-b-PS-*b*-P2VP triblock terpolymers and (b) a 3D TEM tomography reconstructed image. Reproduced from ref 14, with the permission of AIP Publishing.

Another striking example where marked multimodal dispersity was able to produce a very specific morphology by selected chain location was reported by Asai et al.[15] in a 2014 paper. In this work, ISP polymers having the same molar mass (c.a. 120 $kg.mol^{-1}$), the same middle-block volume fraction, but a marked difference in end-block volume fraction (volume fractions of PI:PS:P2VP equal to 0.39:0.56:0.05 and 0.06:0.62:0.32) were mixed. For a binary blend exhibiting an overall PI:PS:P2VP composition of 0.23:0.59:0.18, a tetragonal arrangement of rectangular-shaped rods was formed as proved by SAXS and TEM experiments. The creation of such non-CMC interfaces, with flat edges and sharp corners is unique in the landscape of block polymer morphologies, where round interfaces are preferred. Just like the undulated lamellae, the authors attributed this particular feature to a very specific

spatial arrangement of the block polymers as represented in Figure 1.3: small PI and P2VP blocks are located at the edges of the domains, whereas the larger ones weakly segregate on the corners. These positions of the chains help to stretch the chains and to fill the domains uniformly. In this case, the conformational entropy loss is recovered due to the shape of the interface and the specific placement of the chains. It is worth noting that this tetragonal arrangement of rectangular-shaped rods was recently reproduced in thin films by Guliyeva et al. in a 2018 paper.[16] Making such an unusual morphology in thin film offers an exciting potential for nanopatterning where the need for rectangular-shaped features in a square symmetry is high, since it is more compatible with the device layout design rules of the microelectronics industry. [17], [18], [19] In two following papers,[20],[21] the same group explored the behavior of blends of ISP having a larger window composition and/or different molar mass. All the studied blends mix asymmetric PI-*b*-PS-*b*-P2VP block copolymers sharing the same middle-block size (PS) but different chain lengths of the two end-blocks. This results in blends having a nearly constant PS volume fraction whereas the volume fraction of the end-blocks is gradually changed depending on the blending ratio. It allowed the authors to form a wide gallery of completely new morphologies, including rectangular rods arranged in a 4-fold symmetry but also "rod-like" morphologies having non-constant sizes and shapes, where tiling patterns consisting of triangles and pentagons were observed (see Figure S1-3 and S1-4). In all cases, different sized chains segregate in common domains, sharing the same interface ("weak" localization). Their precise positioning at the domain boundary produces domains with non-classical shapes (squares, or non-circular rods). For specific compositions, a segregation of the smaller P2VP chains in specific domains (strong localization) was however observed in addition, leading to even more complex patterns (See Figure S1-5).

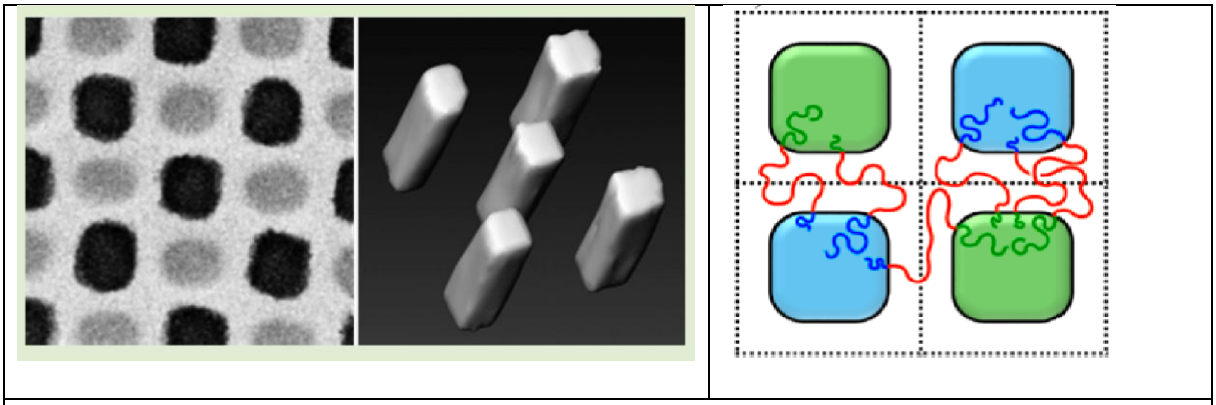

Figure 1-3: TEM image, 3D TEM tomography reconstructed image and the schematic illustration of the morphology observed by Asai et al.[15] for a blend of three symmetric PI-*b*-PS-*b*-P2VP. Reprinted with permission from ref 15. Copyright (2015) American Chemical Society

The property of such blends to form non-uniform domain sizes, and interfaces with a non-constant mean curvature was further exploited to acquire the very unstable double diamond (DD) structure (see Figure S1-6). Again binary blends of two ISP triblock terpolymers with the same total molar mass (c.a. 140 kg.ml^{-1}) but different chain lengths of two end-blocks were used [22]. The chain length ratio between the long and short end-blocks was purposely designed to be large enough (6.6 for PI and 4.7 for P2VP) to fill the center of the 4-fold nodes with longer block chains without further chain stretching. The coexistence of long and short blocks for the two end-blocks results in two interwoven diamond networks of PI and P2VP in a matrix of PS with the long and short blocks filling the nodes and the connectors respectively. This localization of the end-block chains allows for appropriate chain conformations by adjusting long/short chains to wide/narrow spaces, which counterbalances the enthalpy increase due to the increase in interfacial area.

In this series of examples reported by the same research group, PI-*b*-PS-*b*-P2VP was used as a building block in the construction of these unusual morphologies. The high level of incompatibility between all the blocks means that short end-blocks can be used, while preserving the formation of segregated domains containing blocks of different sizes that allows for the stabilization of non-CMC interfaces. Using less incompatible blocks would

have potentially led to solubilization of the smaller blocks in the matrix, ruining the possibility of acquiring a new type of morphology. Blending block copolymers exhibiting a combination of PI, PS and P2VP blocks therefore appears as an interesting way to acquire new types of morphologies, or at least morphologies that are different from the parent ones. This was exploited by Ahn and coworkers[23], using a mixture of a triblock (ISP) (9-63-12 kg.mol^{-1}) (coexistence of spheres and cylinders in tetragonal packing) and a diblock (PI-*b*-PS) (8-70 kg.mol^{-1}) (spherical morphology). In the two copolymers, PI and PS have approximatively the same molar masses.

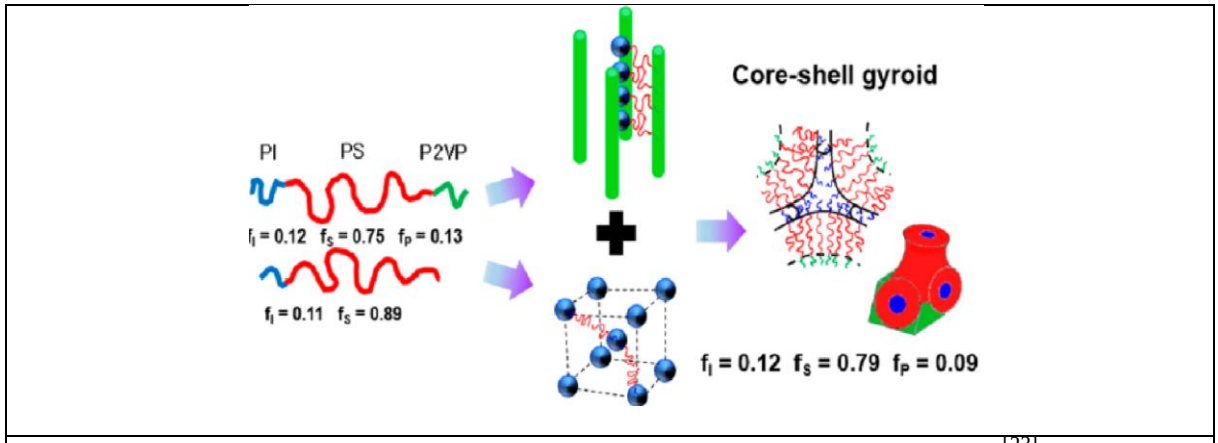

Figure 1-4: Schematic illustration of the morphology observed by Ahn et al. [23] for a blend of PI-*b*-PS-*b*-P2VP and PI-*b*-PS. Reprinted with permission from ref 23. Copyright (2017) American Chemical Society.

The blends of these polymers with a weight ratio from 0.75:0.25 to 0.5:0.5 lead to a core-shell gyroid (core of PI, shell of PS) in a matrix of P2VP as shown in Figure 1-4. As highlighted by the authors, it is very unusual to form a core-shell morphology even at highly asymmetric volume fractions. This goes with the preferential localization of the PI-*b*-PS-*b*-P2VP in the nodes and the PI-*b*-PS in the struts (or connectors). P2VP fills the remaining space and becomes the matrix.

In a rather different approach, Haenelt et al.[24] investigated binary blends of two asymmetric triblock terpolymers with the same type of monomers but different block sequences (ABC, BAC) and block lengths. In this work, two asymmetric polystyrene-*b*-polyisoprene-*b*-

poly(methylmethacrylate)(PS-*b*-PI-*b*-PMMA) (SIM) and polyisoprene-*b*-polystyrene-*b*-poly(methylmethacrylate) (PI-*b*-PS-*b*-PMMA) (ISM) triblock terpolymers were specifically prepared. In both cases, sequential anionic polymerization was used in order to guarantee a reasonably low level of dispersity (< 1.2). Two specific features in this system have to be noted: i) the presence of a small PI block (only 7 monomer units) in the SIM block polymer; ii) a rather moderate repulsive interaction between the PS and PMMA blocks that allows direct contact between the two domains in the (SIM) copolymer. Blends containing various fractions of SIM (171 $kg.mol^{-1}$, double gyroid) and ISM (95 $kg.mol^{-1}$, cylindrical morphology) were prepared, forming morphologies that differ from the parent polymers. In particular, they were able to produce new ISIM tetrablock terpolymer-type morphologies such as double gyroid, cylindrical and spherical structures. The only explanation for such structures is that PS and PMMA blocks of both triblocks mix into each other (thereby reducing the packing frustration) whereas the PI forms separate isolated domains (Figure S1-7).

It is important to note that these intriguing morphologies (in the case of either the diblock or the triblock) result from the absence of macrophase separation (i.e. the blocks with the same chemistry remain miscible at the molecular level). Micro vs macrophase separation competition was firstly addressed, both experimentally [25],[26] and theoretically [27] on binary blends of a diblock and a homopolymer. It was demonstrated that the addition of homopolymer A in diblock A-b-B is first driven by the relative molar mass of the components. If M_{hA} (molar mass of the homopolymer A) is less than M_{bA} (molar mass of the A block), a wet brush regime is observed with hA (homopolymer A) dispersed in bA (block A) or localized at the center of the phase. In contrast, if M_{hA} is greater than M_{bA}, macrophase separation occurs. Avoiding phase separation also implies conditions on the volume fraction of homopolymer. Typically, Tureau [28] concluded that a fraction less than 0.30 of homopolymer is required to avoid macrophase separation for a binary blend of triblock

copolymer and homopolymer. Conditions for homogenous blends were also examined in diblock copolymer blends. Again, the molecular weight differences between the components and their volume fraction are critical. For example, Matsen[29] calculated the phase separation between two symmetric diblock blends and found that macrophase separation occurs if the chain length ratio of long diblock to short diblock is larger than 5, and the volume fraction of short copolymer larger than 0.2. Another interesting simulation study by Wu et al. in 2010 [30] concerned the phase behavior of binary blends of a long symmetric AB diblock copolymer and a short asymmetric AB, where macrophase separation occurred when the chain length ratio was large enough (ca. 5.3).

Self-assembly model and chain location

In all these examples, the authors assumed a specific localization of chains (or junctions) around interfaces in order to explain the non-classical morphology obtained. For example, in the diamond structure obtained with the PS-b-PI blend, it is proposed that the long chains of PI selectively fill the thicker connections (nodes), whereas short chains occupy the channels (see Figure 1.1). In the PI-*b*-PS-*b*-PVP blend, small PI and P2VP blocks are assumed to be located at the edges of the domains, whereas the larger ones segregate on the corners. Although these models were based on reasonable arguments (considering the energy balance between translational entropy, amount of interface, conformational entropy, and packing frustration), no real experimental evidence has yet been provided or calculations undertaken in order to fully confirm these assumptions.

Concerning the specific positioning of the chains around the interfaces, this could be experimentally investigated by neutron reflectivity of partially deuterated systems, based on the work by Koneripalli[8] or Noro[11]. In Koneripalli's work, using binary blends of PS-*b*-P2VP symmetric diblocks of different molar masses (58 -120 $kg.mol^{-1}$), or asymmetric

diblocks with different volume ratios of P2VP but the same molar mass (20 kg.mol^{-1}), they demonstrated that these blends all exhibit a lamellar structure parallel to the surface. The long PS chains are located in the centers of the domains whereas the short chains are located at the domain boundaries. In Noro's work, they also investigated the location of copolymer chains as a function of their length in thin films of ternary blends of P2VP-*b*-PS diblocks and also of P2VP-b-PS-b-P2VP triblocks. The diblocks or triblocks had the same molar mass (100 kg.mol^{-1}) but different volume fractions of PS, where merely one species out of three was selectively deuterium-labeled. All the resulting blends exhibited a lamellar structure. Using neutron reflectivity measurements, they investigated the chain distribution and the interfacial thickness. The conclusions reached are the same as those of Koneripalli, with the localization of the short chains near the interface of the domains and of the long chains at the centers of the lamellae. They also showed that the interfacial thickness depends on the chain distribution of blocks.

One of the main outcomes from the review of the literature concerning these multimodal blends of copolymers is the paucity of theoretical studies to understand the formation of these morphologies. In contrast, accessible morphologies have been confirmed or predicted for neat diblocks and triblocks [31] using theoretical calculations such as Self Consistent Field Theory (SCFT).[32],[33] Calculations concerning blends are much more limited and concern simple blends.[34] An important research avenue would therefore be to develop simulation in order to predict the morphology for a given blend composition. This will in turn facilitate the design of block copolymers and the selection of their blending ratios in order to obtain a desired morphology. A method for that purpose was proposed using "Swarm intelligence optimization" and tested recently by Paradiso et al. on the basis of SCFT calculations for blends of triblocks under lateral confinement (Figure S1-8).[35] However, the agreement between this prediction and the experimental results has not yet been tested. Moreover, the

distribution of the chains over the pattern has not yet been fully described. Table S1 in the supporting information provides the experimental parameters of the examples described in this section such as block length ratio and polydispersity of the blocks that would need to be taken into account for such an approach.

Conclusion

Using blends of block-copolymers having a multimodal dispersity of the targeted block(s) allows for the creation of "non-classical" morphologies. In this type of macromolecular system, the distribution of the chains for the given targeted block(s) around the interface is not random, i.e., the block junctions are distributed heterogeneously along the interfaces. As a result, non-classical morphologies such as double diamond networks, undulated lamellae, domains with flat surfaces and sharp corners, whose domain interfaces possess the common feature of "non CMC interfaces", have been created. These unusual morphologies have been obtained mainly because the molecular systems design responds to the strong need for the targeted block chains to gain conformational entropy by admitting surface area enhancement and loss of translational entropy for block junction points. This is in good contrast to what we will now describe in the following sections, where junction-free interfaces can be formed.

Part2: Three-arm star terpolymers and related systems

Introduction

In the common sense, block copolymers are in the class of complex polymers in which two chemically different block chains are connected at their junction point in a 1:1 fashion. If we restrict ourselves to A/B two-component systems, AB diblock, ABA triblock and $(AB)_n$ multiblock copolymers are known for linear chains, while A_nB_n type stars or $(AB)_n$ type stars can join when the scope is spread to star-branched block copolymers. When the number of components increases, we encounter ABC and ABCD linear polymers. To summarize the molecular architecture of these molecules, the different chemical species are still connected in a 1:1 fashion, and hence the frustration on block copolymer chains is not as high.

On the contrary, if three incompatible polymeric chains with different chemical species are combined at one connecting point, the ways in which these molecules self-assemble in the condensed state may be dramatically different from the self-assembly patterns of linear molecules. In short, their junction points have to be on one-dimensional trails, either straight or curved, to share three-dimensional space, where individual chains are forced to be located under fairly frustrated (constrained) conditions. This section deals with the self-assembly patterns of ABC three-arm molecules, where the A, B, and C components need to be sufficiently incompatible with one another.

Various types of self-assembled patterns in three-arm star terpolymers

Experimental approaches and theoretical calculations as well as simulations on this frustrated system started around the same period, in the 1990s. We will first review these studies from the experimental point of view, in which the first stage is the synthetic pathways of these very complex molecules. It is obvious that polymer/polymer coupling reaction(s) is(are) needed to produce a three-branched architecture having three different polymer arms in a “living”

fashion. Therefore, highly purified experimental set-ups are required. Anionic polymerization under high vacuum is probably the most suitable method for the synthesis of polymers with well-defined molecular structures. In addition, it is a good synthetic strategy to adopt the chemistry of diphenylethylene by using the chemical reaction characteristics of this type of monomer, namely: 1) this monomer cannot polymerize itself anionically, but 2) the living end of this chemical moiety can initiate and polymerize some vinyl monomers. Fujimoto et al. introduced diphenylethylene chemistry into anionic polymerization reactions under vacuum and they succeeded in preparing polystyrene/polydimethylsiloxane/poly(tert-butylmethacrylate).[36] Stadler et al. also adopted diphenylethylene chemistry and prepared polystyrene/polybutadiene/poly(methylmethacrylate) three-arm molecules [37] whereas Hadjichristidis et al. synthesized polyisoprene/polystyrene/polybutadiene three-arm molecules by using a chlorosilane chemistry.[38],[39] It should be stressed that this involved extensive purification and isolation work because the reaction yields were quite low in all cases.

The second stage from the experimental point of view was studies on self-assembled structures which are clearly different from those of linear ones because of the branched chain architectures. This class of molecules tends to form more or less anisotropic morphologies composed of cylinders or rods because of this spatial restriction, whose domain interfaces mostly show the surface feature of non-CMC. Therefore, reports focused on two-dimensional patterns such as cross-sectional views of cylinder/rod assemblies. Huckstadt et al.[40] found several cross-sectional periodic patterns from polystyrene/polybutadiene/poly(2-vinylpyridine) star-block terpolymers, while Yamauchi et al.[41],[42] reported similar structures from a polystyrene/polyisoprene/polydimethylsiloxane material system, in which polymer/polymer interfacial curvatures were not exactly constant. Furthermore, Sioula and coworkers succeeded in finding periodic tiling patterns from polystyrene/polyisoprene/polymethylmethacrylate (SIM) three-arm star molecules, in which

one is co-axial rods having a PI core with a PS shell embedded in a PMMA matrix from a molecule with molar masses of 72/77/144 kg.mol^{-1} for PS, PI, PMMA, respectively, the other is a pattern with 6-fold symmetry from a molecule with the molar masses of 92/60/94 kg.mol^{-1}. It was confirmed by TEM observation that the two molecules exhibited highly periodic two-dimensional patterns with non-CMC domain interfaces, as shown in Figure 2-1.[43]

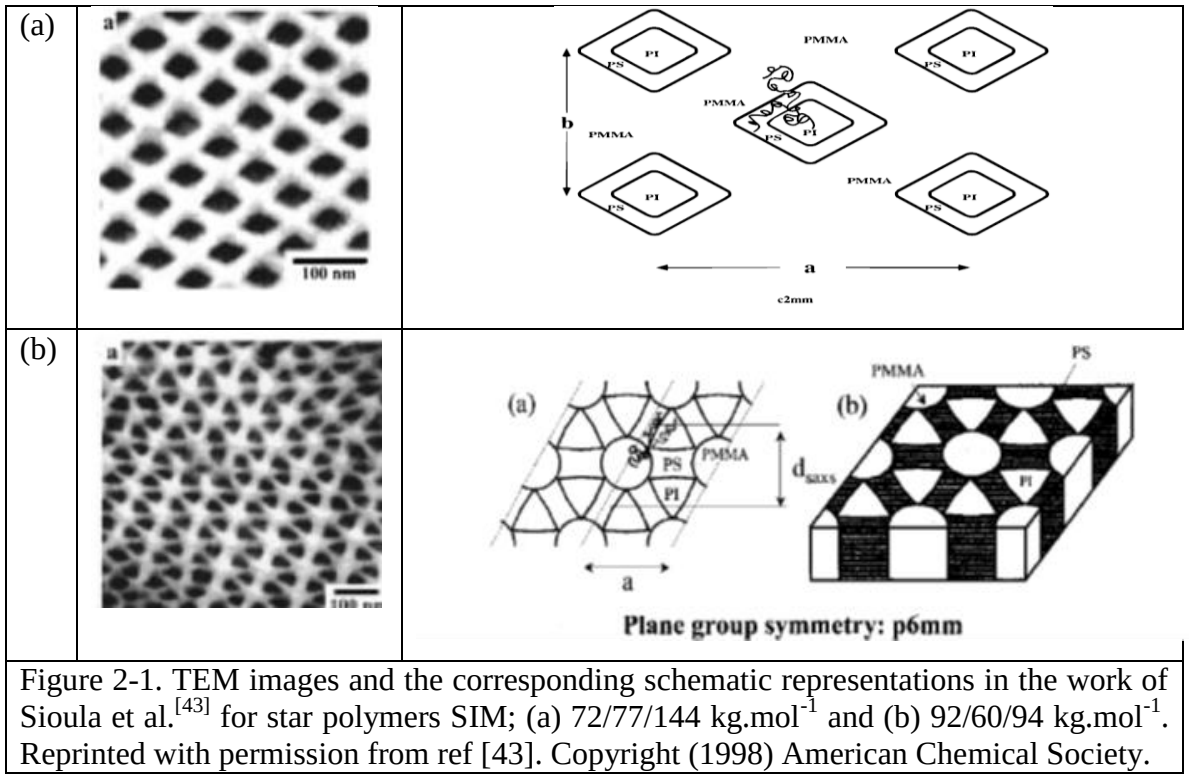

Figure 2-1. TEM images and the corresponding schematic representations in the work of Sioula et al.[43] for star polymers SIM; (a) 72/77/144 kg.mol^{-1} and (b) 92/60/94 kg.mol^{-1}. Reprinted with permission from ref [43]. Copyright (1998) American Chemical Society.

On the other hand, the results from simulation approaches were somewhat more conclusive than the experimental ones in the early stage. Compared to the other two systems studied in this review (Part I and III), star block copolymers are homogeneous systems (i.e. one component) that makes a theoretical approach more readily available. In a pioneering simulation study on the two-dimensional space filling problem, Dotera and Hatano[44] reported a tiling pattern for the self-assembly of ABC-star molecules by adopting a diagonal bond method of a Monte Carlo simulation. This was followed by extended work on a series of molecules of the type $A_1B_1C_X$ (X is merely the variable), where systematic transition among tiling patterns composed of the tessellation of even-numbered polygons, i.e., (4.8.8), (6.6.6),

(4.6.8) and (4.6.12), was clearly represented depending on X for the first time (See Figure S2-1).[45] Though the particular term of "Archimedean tiling"(AT) [46] was not used in their study, in fact many of the obtained structures satisfy the geometrical features of AT patterns, as shown in Figure 2-2. Moreover, Bohhot-Aviv and Wang[47] carried out theoretical calculations for the same type of molecules based on a Self-Consistent Field (SCF) approach. By varying the magnitude of interaction parameters they found the (6.6.6) AT pattern among several periodic patterns (See Figure S2-2), whereas Tang et al. reported on many periodic patterns including (6.6.6), (4.8.8) and (4.6.12) AT formations for ABC stars by SCF calculation.[48] Using DPD (Dissipative Particle Dynamics), Kirkensgaard[49] showed that a very diverse landscape of morphology could be envisioned by increasing the number of arms. A good number of recent papers [50],[51] confirm the strong interest of simulation in star block copolymer research in modern polymer science.

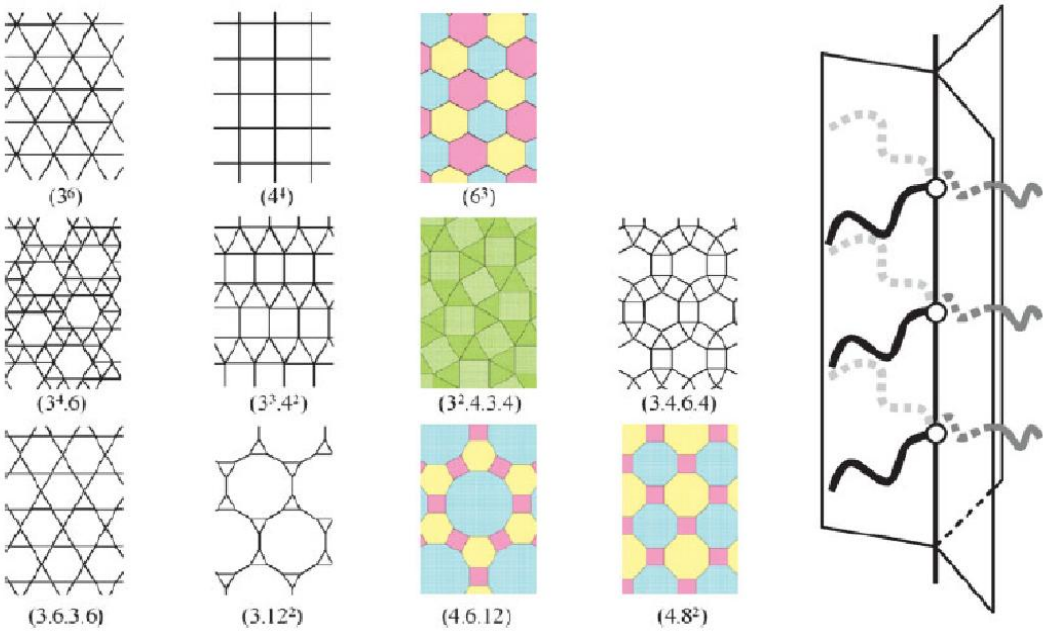

Figure 2.2 Eleven possible Archimedean tiling patterns and schematic alignment of ABC star-shaped block terpolymer molecules in a molten state as proposed by Takano et al.[51] Reprinted from ref [51] by permission of John Wiley & Sons, Inc. Copyright © 2005 by John Wiley Sons, Inc.

The third stage from the experimental aspect was the finding of distinct tiling patterns. The patterns can be sensitively tuned by the relative chain lengths, and consequently many of them can be categorized as AT. In fact, if the relative chain lengths in a molecule are not very different from one another, the junction points can be aligned on a straight line, forming columnar domains. Their cross sections naturally reveal two-dimensional tilings from polygons because domain interfaces are mostly flat due to the restricted condition: no junction points on the interfaces, where even the concept of non-CMC cannot be applied.

Takano and coworkers prepared a series of polyisoprene/polystyrene/poly(2-vinylpyridine)(ISP) three-arm molecules of the type $I_1S_1P_X$ ($0.7 \leq X \leq 1.9$) based on diphenyl-ethylene chemistry, and investigated the structures of the cast and annealed bulk films. A systematic change in morphology among the AT was reported, which includes (6.6.6), (4.8.8), (4.6.12) AT with 3-fold, 4-fold and 6-fold symmetry, at X of 0.7, 1.2 and 1.9, respectively as can be seen in Figure 2-3.[52] In this figure, another more complex but still periodic (3.3.4.3.4) AT is shown at X of 1.3, where the periodicity can be recognized by superimposing triangle/square tiling on the TEM image as shown in the figure by red auxiliary lines. This complex but periodic structure was actually created from the binary blend of two molecules with X equal to 1.2 and 1.9. These two molecules were weakly localized in this newly-found structure in order to relax frustration.

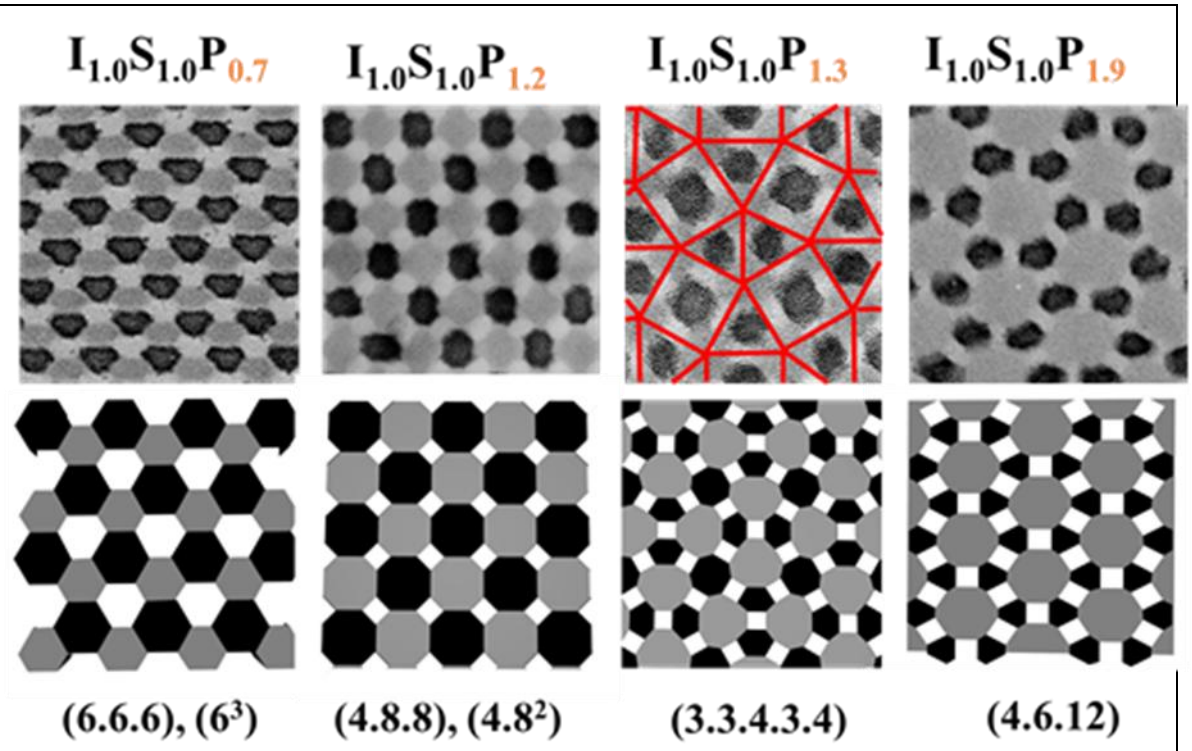

Figure 2.3 Four types of Archimedean tilings, i.e. (6.6.6), (4.8.8), (3.3.4.3.4) and (4.6.12), appearing in three-arm star molecules of the $I_{1.0}S_{1.0}P_X$ type. TEM images are at the top and the schematics are at the bottom.[52]

Successively, Hayashida and coworkers investigated the structures for different series of ABC-star molecules using the same chemical components: $I_1S_YP_2$ (Y is merely the variable composition parameter this time), where ATs were again observed. Among them, the (3.3.4.3.4) structure was designed with the sample of $I_1S_{2.3}P_2$.[53] By blending low molar mass S and P homopolymers into this copolymer and when the composition reaches $I_1S_{2.7}P_{2.5}$, the blend shows a somewhat more complex structure without periodicity. By careful structure analyses, a quasicrystalline tiling was proved by both TEM observation and X-ray diffraction, as shown in Figure 2-4.[54] This structure has a tile size of more than 50nm, which is larger than that derived from a metal-alloy (0.5nm), a calcogenide (2nm) and a dendrimer (10nm) and it is the first-found quasicrystalline tiling in soft materials. Periodic two-dimensional patterns were also found and reported by Ross and coworkers from polystyrene/polyisprene/polyferrocenylsilane star terpolymers (PS/PI/PFS).[55],[56] Among

them, two ATs, i.e. (4.8.8) from the molecule of 0.43/0.34/0.23 and (4.6.12) from the molecule of 0.37/0.40/0.23 were found. Furthermore, many featured worm-like structures were created from polyethylethylene/polyethylene oxide/polyperfluoropropylene star-molecules in aqueous solutions. [57],[58]

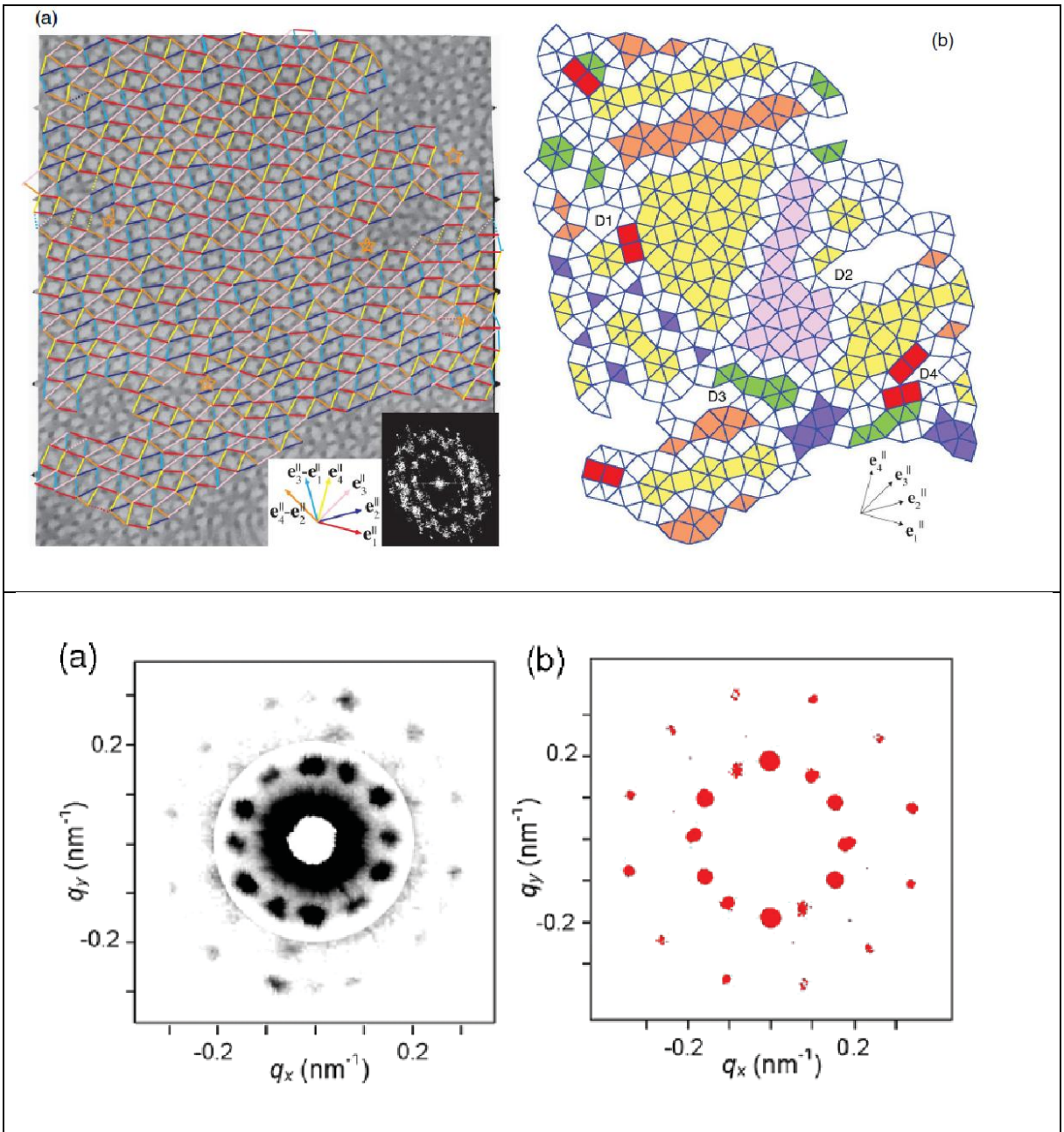

Figure 2.4: A wide-view TEM image with a triangle-square tiling, schematic representation and microbeam small-angle x-ray scattering pattern in Hayashida et al.[54] for a $I_{1.0}S_{2.7}P_{2.5}$ star block polymer/homopolymer blend. Reprinted figures with permission from ref [54]. Copyright (2007) by the American Physical Society.

Conclusion

3-arm star molecules of the ABC type easily form anisotropic cylinder/rod morphologies, in which many of the cross-sectional views show the characteristics of two-dimensionally periodic Archimedean Tiling (AT) structures. These results come directly from the constrained location of their junction points, i.e., they need to be on one-dimensional lines, either straight or curved, resulting in producing "non-classical" morphologies with flat interfaces and sharp corners. As an exceptional extension of the morphological study of this molecular system, star molecules can even form quasicrystalline tiling with dodecagonal symmetry so as to relax molecular frustration.

Part3: Self-assembly of block polymers coupled with supramolecular interaction

Introduction

Generally, most of the microphase-separated phases include only one chemical species each, particularly in the strong segregation regime. In fact, if a system is composed of merely amorphous and nonfunctional polymer chains, no distinct forces are generated among chains except van der Waals interactions. In contrast, when polar species or functional groups are introduced into the system, some additional interactions can be naturally generated in the individual phases, and may strongly influence the structure formation. For example, hydrogen-bonding interactions can be easily introduced between block chain and counterpart molecules, whose size ranges from small chemical molecules to homopolymers and even to whole block chains in a block copolymer. Small molecules and homopolymers can have similar effects on structure formation, i.e., they more or less play the role of increasing the volume of the host polymer phase, and hence they can cause morphological transition. The situation is very different, however, in the case of block copolymer/block copolymer blends, in which hydrogen-bonding moieties are included in one block chain of one copolymer. In short, two polymer species can cooperatively interact together in solution to form hydrogen bonding, and the interaction can be kept if the concentration of the solution increases and even in bulk state, resulting in giving one homogeneous complex phase from two totally different chemical species. The restrictions on chains are considerably different from those of the simple block copolymer system and also of block copolymer blends without particular interactions. The former polymer system is known to form featured self-assembled structures, which have never been observed in pure block copolymer systems. This section mostly deals with this type of molecular assembly and concludes with block copolymer blends.

Blend of block copolymer with small molecules

Ruokolainen and co-workers[59],[60] in their pioneering work found a hierarchical periodic structure with two periodicities from the combination of a block copolymer/low molar mass compound, i.e., polystyrene-*b*-poly(4-vinylpyridine)(PS-*b*-P4VP) diblock copolymer and pentadecyl phenol (PDP). PDP was hydrogen-bonded with a 4-vinylpyridine unit and the straight PDP molecule hung on the P4VP unit to align orderly, forming short lamellae oriented perpendicular to large lamellae of the block copolymer itself. This system can form a hierarchical structure with two length scale periodicities. PDP chains in the alternating PV4P/PDP lamellar domains are in a highly restricted situation and their chain dimension along the transverse direction can be severely limited due to the PDP hanging on their pyridine ring moieties. In other words, PV4P/PDP hydrogen bonding can produce small lamellae in the mixed domain, and PDP molecules can compensate the chain dimension of PV4P, so as to balance the dimension of PS in this direction. Consequently, PV4P/PDP short lamellae can be formed and asymmetric lamellar structures are also created. Thus, the introduction of hydrogen bonding between functional moieties in a block chain and small molecules can even induce restriction of block copolymer junctions on the microdomain interface. The structural feature was clearly demonstrated by transmission electron microscopy combined with X-ray diffraction experiments, as shown in Figure 3-1. Furthermore, Kuila and Stumm studied the supramolecular assembly of polystyrene-b-poly(4-vinylpyridine) diblock copolymer/small molar mass compounds such as 2-(4'-hydroxybenzeneazo) benzoic acid (HABA), 1-pyrenebutylic acid (PBA) and ferroceneacetic acid (FAA) interacted with hydrogen bonding in thin films and found several featured nanopatterns.[61]

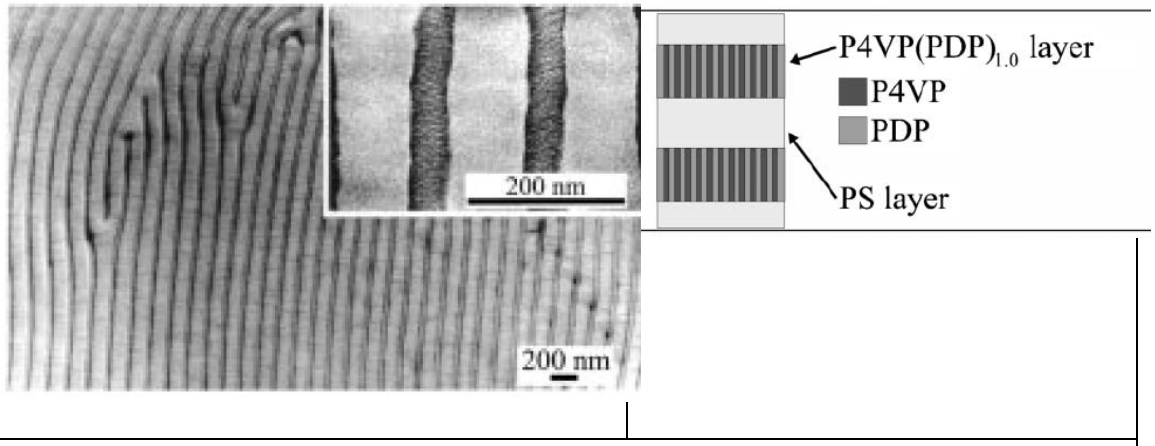

Figure 3-1: TEM image of a hierarchical structure formed by a blend of PS-b-P4VP diblock copolymer and PDP[60] (reprinted with permission from ref [60]. Copyright (1999) American Chemical Society) and corresponding schematic representation in Ruokolainen [62] (reprinted with permission from ref [62]. Copyright (2007) Royal Society of Chemistry.)

Block copolymer/homopolymer blends

There are plenty of examples of block copolymer/homopolymer blends adopting a homopolymer of the same chemical species as in the block copolymer, but they are not mentioned here because the main focus of this sub-part is hydrogen bonding interaction in self-assembled block copolymers. Dobrosielska et al.[63] observed a systematic morphological transition in a polystyrene-*b*-poly(2-vinylpyridine)(SP)/poly(4-hydroxystyrene)(H) diblock copolymer /homopolymer blend formed in toluene/hexane mixed solvent. A large amount of H homopolymer can be homogeneously mixed into the microphase-separated poly(2-vinylpyridine) phase beyond the stoichiometric amount and plays a role similar to that of a simple homopolymer of the same polymer species as in block copolymer chains (see Figure S3-1). Here very interestingly, the added homopolymer can even cause a morphological transition that is not observed in the case of classical block copolymer/homopolymer blends. Thus, the morphology is much more easily tunable for block copolymer/homopolymer blends with a hydrogen-bonding system than for blends without hydrogen bonding because a large amount of homopolymer can be dissolved in block chains, causing a morphological transition due to a volume fraction imbalance. This gives a new and easy morphology control method

by varying the circumstances of two block chains conforming interfaces where block junction points stand.

Block copolymer blends

There have been many attempts at morphology control with blends of block polymers bearing hydrogen-bonding moieties. Among the pioneering studies, Jiang et al.[64] observed a periodic but complex structure with double periodicity in polystyrene-b-polybutadiene-b-poly(tert-butylmethacrylate) (SBT), where 18% of methacrylate units were hydrolysed and transformed into methacrylic acid (A) units, and a polystyrene-b-poly(2-vinylpyridine)($S_{45}V_{55}$) binary blend. Because of the hydrogen bonding between A and V units, these two blocks can mix at a molecular level, and hence the formation of an ordered superlattice structure with double periodicity bearing three phases was found. The three phases were confirmed by selective staining using three staining agents (OsO_4 for B, CH_3I for mixed complex phase (V+T/A), and RuO_4 for S phase) revealing a very complex but periodic phase structure with two periodicities by TEM (Figure 3-2).

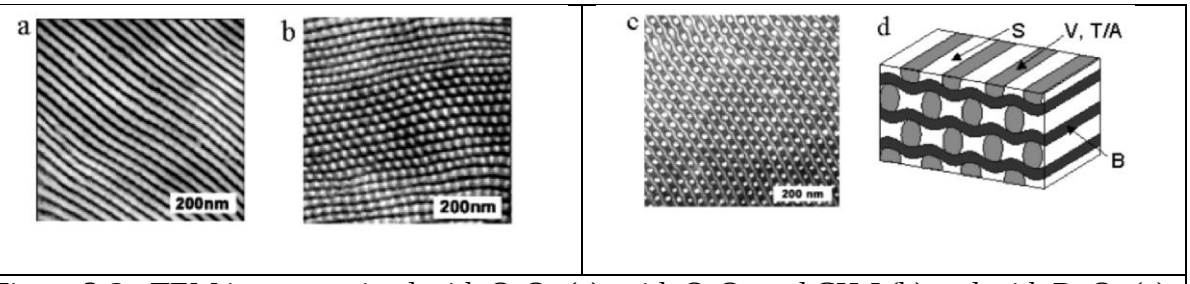

Figure 3-2 : TEM images stained with OsO_4 (a), with OsO_4 and CH_3I (b) and with RuO_4 (c) and a schematic representation (d) in Jiang et al. for SB(T82/A18) blend with $S_{45}V_{55}$ [64]. Reprinted with permission from ref [64]. Copyright (2003) American Chemical Society.

Meanwhile, Asari et al. [65] carried out an interesting attempt to show the difference in the manner of structure formation with/without hydrogen bonding. In their work, a block copolymer blend of polystyrene-*b*-poly(4-tert-butoxystyrene))(StB, volume fraction of tB 0.14) and polyisoprene-*b*-poly(2-vinylpyridine) (IP, volume fraction of P 0.09) with relative ratio 50/50, exhibited a macrophase-separated structure as shown in Figure S3-2a. In contrast,

the blend of polystyrene-*b*-poly(4-hydroxystyrene))(SH) and IP (the former was obtained by hydrolysis of StB) revealed a clear microphase-separated structure as if it were formed by a simple SI diblock copolymer (Figure S3-2b). Due to hydrogen-bonding interaction between H and P, these two polymer chains can mix to produce a simple phase, forming cylinders periodically aligned on the lamellar interface of S and I as shown in Figure 3-3a[66], where the hierarchical morphology was clearly observed in this asymmetric SH/IP blend. If the fractions of H in SH and P in IP increase and both reach 50% (volume fraction of H in SH and volume fraction of P in IP equal 0.50), the P/H mixed phase forms independent lamellae, while S and I phases are aligned alternately in adjacent lamellar domains as shown in Figure 3-3b. In both cases, the S/I domain boundary, which is associated with the white/black boundary in the TEM image, is flat because there are no junction points in between the S/I interface; all the junction points are located at the I/(P+H) interface on one side and the S/(P+H) interface on the other side. Again, this can be seen as a constrained location of the junction points which, in turn, is responsible for the formation of this "non-classical" morphology. It is worth noting that such complex hierarchical morphologies are not always formed when mixing AB and CD block copolymers, where B and C blocks are compatible through hydrogen bonding. For example, Chen and al.[67] observed a simple three-phase lamellar structure in a polycaprolactone-*b*-poly(4-vinylpyridine)(PCL-b-P4VP)/polystyrene-*b*-poly(vinylphenol)(PS-*b*-PVPh) blend. Here the blend behaves like a simple ABC triblock linear terpolymer of PCL-*b*-P4VP/PVPh-*b*-PS, where P4VP/PVPh is a mixed phase (see Figure S3-3).

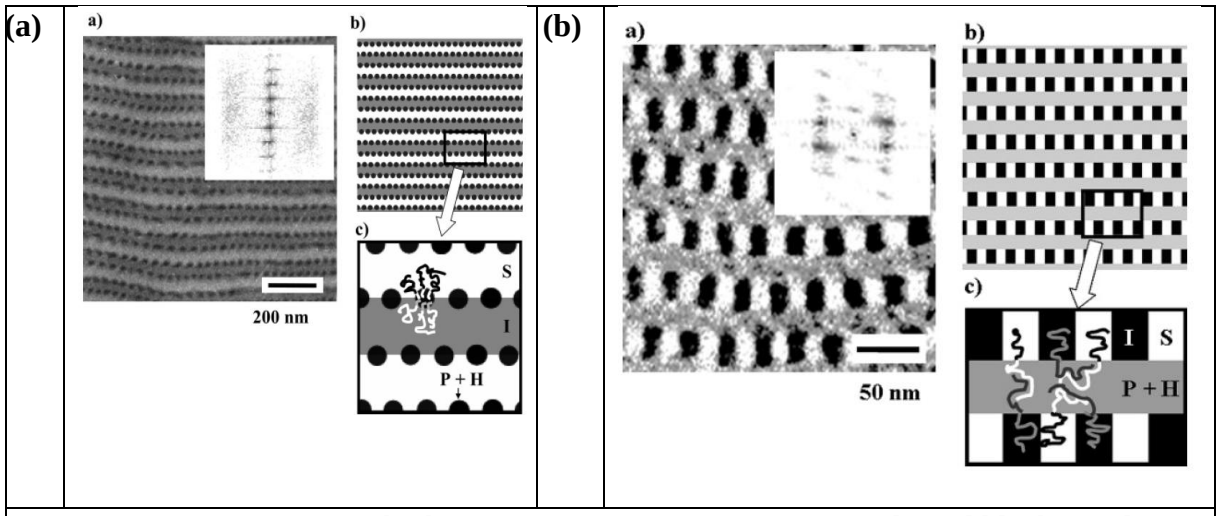

Figure 3-3: TEM images and schematic representations in Asari et al. on diblock copolymer blend films for (a)IP-91/StB-91 = 50/50 and (b)IP-55/SH-55 = 50/50 blends.[66] Reprinted with permission from ref [66]. Copyright (2005) American Chemical Society.

Even more complex patterns were obtained using mixtures of ABA triblocks and CD diblocks, where intermolecular association via hydrogen bonding between components A and D gave various kinds of supramolecular structures, since some fractions of ABA molecules adopt a bridge conformation.[68] Resulting from this constrained self-assembling, the system was confirmed to form triangle and square "non-classical" closed-loop patterns (see Figure S3-4a). Using this strategy, several new Archimedean tiling structures were found in a poly(2-vinylpyridine)-*block*-polyisoprene-*block*-poly(2-vinylpyridine)/poly(styrene)-*bloc-poly(*4-hydroxystyrene) PIP/SH triblock/diblock blend system (see Figure S3-4b), where P and H blocks mixed at a molecular level. This highlights that the fraction of hydrogen-bonding moieties is a very sensitive factor to give final stable structures in bulk. In the example of Figure S3-4b, I/S flat interfaces with no junction point were created, all the block junctions, i.e. P-I and S-H, being located at the boundaries between the (P+H) mixed phase and the I or S phases.

As an extension of diblock polymer blends, some advanced studies including triblock copolymers of the ABA type were carried out. Mather et al. [69] investigated the structure formation of two triblock copolymers of the ABA and CBC type, where B denotes the

common block chain of poly(n-butyl acrylate) and A and C represent derivatives of polystyrene with adenine(A) and thymine(C) side groups as hetero-complementary units to form multiple hydrogen-bonding. As a result, the blend of ABA and CBC gave two representative morphologies in thin film state: cylinders oriented horizontally and perpendicularly to the surface of the substrate. This molecular system can form complemental hydrogen-bonding in solution so as to enhance solution viscosity, and hydrogen-bonding can be stable in bulk to give a higher softening temperature of the material. The latter phenomenon was probably due to the high fraction of bridge conformation of block chains, in which two end-blocks stay in the different microdomains owing to the molecular design employed.

Another interesting trial was conducted on an ABC star-shaped molecule/DE diblock copolymer blend, where components C and D can form hydrogen-bonding. Miyase and coworkers investigated the structure of a blend of an ISP-star molecule (I polyisoprene, S polystyrene, P poly(2-vinylpyridine)) and HM (H poly(4-hydroxystyrene), M poly(methylmethacrylate)) diblock copolymer, whose P and H chains are very short. They found a complex but very periodic structure.[70] By rinsing out HM diblock copolymer molecules in acetic acid-methanol mixed solvent, it was found that the unit cell of the periodic structure with a 5-coordinated domain assembly is a large hexagon, whose side length is longer than 100 nm (which is much longer than the domain size of individual block chains). This phenomenon resembles that of the binary blend of ABC triblock terpolymers with different block chain lengths discussed in part 1 in this article, meaning that block chains in the present system are in a constrained situation (see Figure S3-5).

Conclusion

Various new self-assembled structures can be created in blends of block copolymers by introducing intermolecular association through hydrogen bonding between selected blocks in the block copolymers and compensative counterparts in small molecules, homopolymers or another block chain. By specifically designing the block copolymer architecture, focusing especially on the position of the blocks in the copolymer that will undergo intramolecular association, constraints or frustrations arise depending on the placement of the chains (including a closed-loop situation), allowing for the formation of "non-classical" morphologies. As a result, non-CMC boundaries with flat interfaces and sharp corners can be formed. The features of these boundaries obviously differ from the usual phase behavior of linear block copolymer systems.

General Conclusion and Future Perspectives

In any self-assembled block copolymer morphology (i.e. below the order-disorder transition), the location of the chains and junctions is in fact not random and already displays some levels of restriction in their placement. In this review, we have detailed the consequences of an increased level of constraint in the location of the chains and/or junctions on self-assembled morphologies. This has been highlighted for three categories of systems: multimodal blends of block copolymers, star block polymers, and supramolecular assemblies. A common feature of these three systems is that they have (compared to a simple self-assembled linear architecture) a more constrained distribution of their chains and/or junctions around the interface (junction-free interfaces can even be formed) that allows for the creation of "non-classical" morphologies. Particularly, the opportunity to create domains with flat surfaces and sharp corners is a very interesting and distinct feature of this kind of "frustrated" system. This specific behavior mainly arises from the use of structures created by contrived molecular design, where in most cases, each individual block has a very narrow molar mass and composition distribution.

As future perspectives, we firstly think that there is still plenty of room for creating new unexpected morphologies, using the strategies detailed in this review, but using different chemistries of the blocks. For example, if we take the multimodal disperse blends of block copolymers, most of the examples reported are based on I, S and P. It can be easily anticipated that some other different material compositions would change the interaction parameters and the blocks' flexibility that will in turn modify the equilibrium morphology. Secondly, we demonstrated in this review a lack of structural prediction using theoretical calculations. This is particularly true in the case of blends where simulation would be relevant to predict the block copolymer compositions and their blending ratios in order to obtain a desired morphology of the system. Lastly, we strongly believe that the thin film version of

this type of morphologies offers an exciting potential for surface nanopatterning. However, only a few studies have so far demonstrated that it is actually possible, highlighting the difficulty of controlling such morphologies in a confined environment. We hypothesize that the delicate and precise assembly reached in such complex systems is easily destabilized at the film interfaces. Surface segregation in particular will play an important role in energy minimization, which in turn will have an effect on the bulk composition. This requires more work to decipher the self-assembly of such systems in a thin film configuration, and more work to precisely control the formation of their domains.

Supplementary Information

Figure S1-1

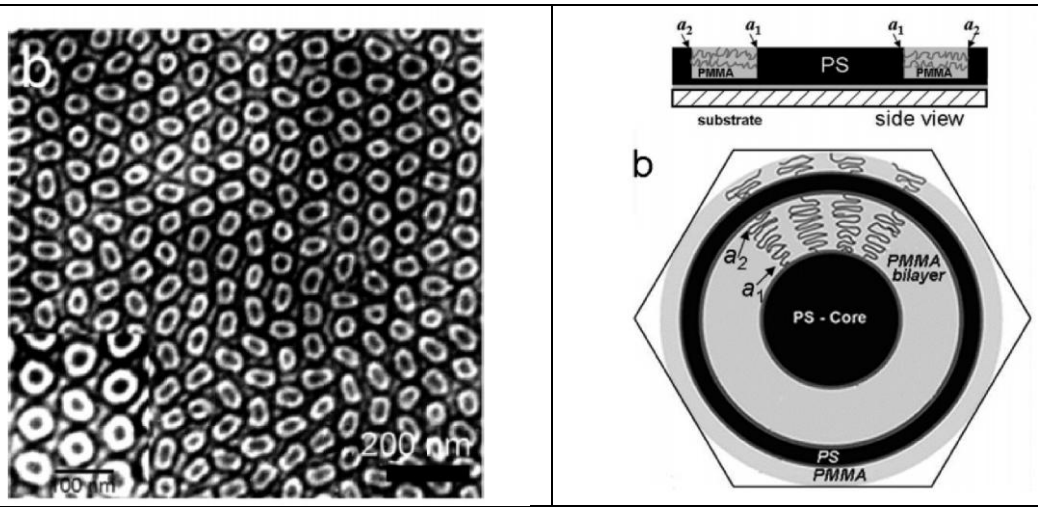

Figure S1-1: (a)TEM image and (b) schematic illustration of the morphology observed by Chen et al. [12] for a blend of two PS-*b*-PMMA. Reprinted with permission from ref 12. Copyright (2006) American Chemical Society.

Figure S1-2

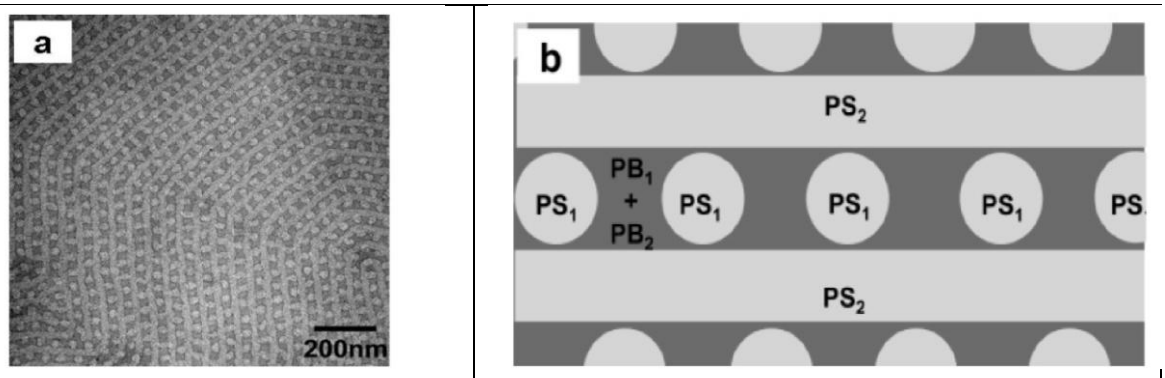

Figure S1-2: (a) A TEM image and (b) the corresponding schematic illustration of the morphology observed by Guo et al.[13] for a blend of the two asymmetric PS-*b*-PB with a 0.5/0.5 weight ratio. Reprinted with permission from ref 13. Copyright (2008) American Chemical Society.

Figure S1-3

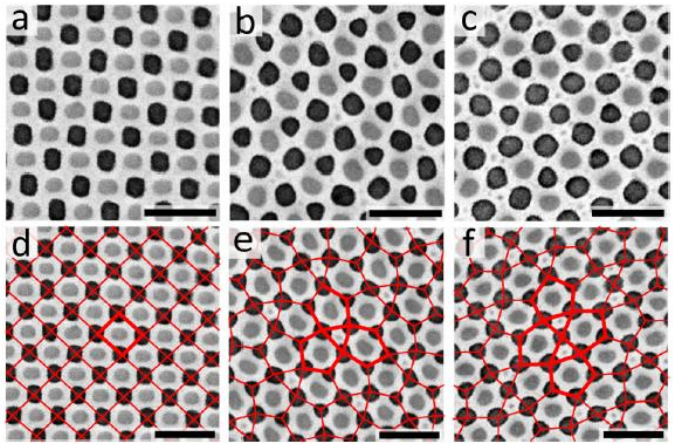

Figure S1-3: TEM images and the corresponding symmetries of triblock blends based on PI-*b*-PS-*b*-P2VP observed by Asai et al.[20] Reprinted with permission from ref 20. Copyright (2015) American Chemical Society.

Figure S1-4

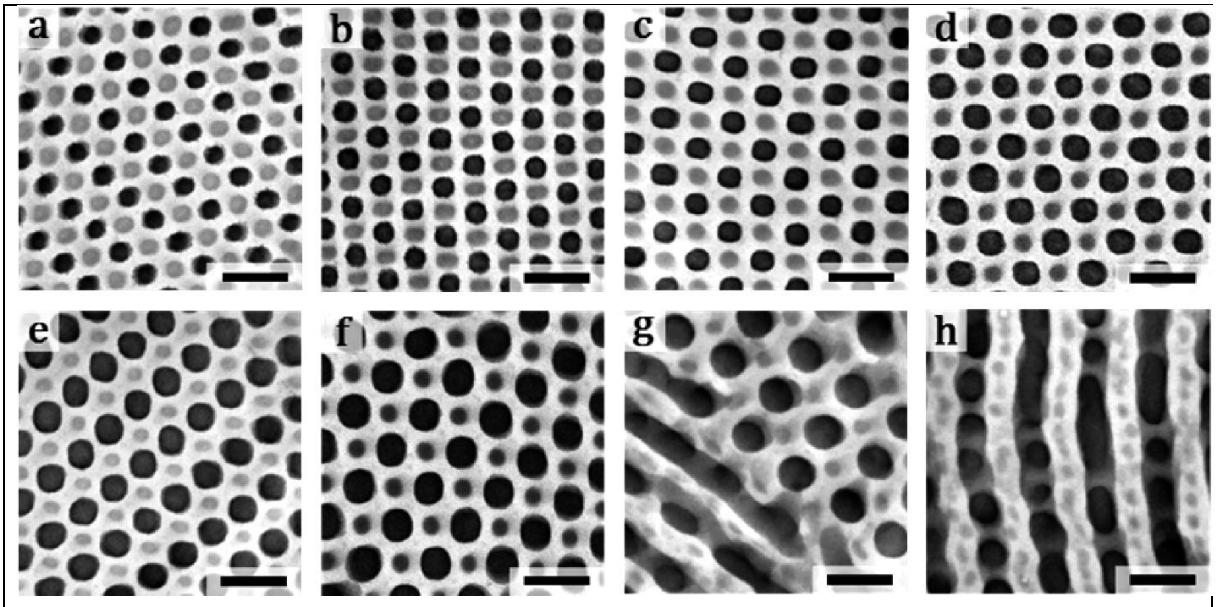

Figure S1-4: TEM images of triblock blends based on PI-*b*-PS-*b*-P2VP observed by Asai et al.[21] Reprinted with permission from ref 21. Copyright (2016) American Chemical Society.

Figure S1-5

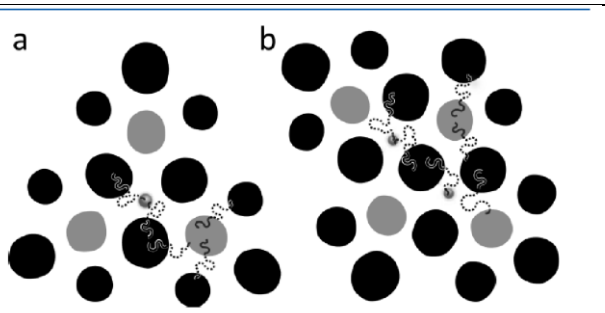

Figure S1-5: Schematic illustration of two morphologies observed by Asai et al.[20] for blends of two PI-b-PS-b-P2VP. Reprinted with permission from ref 20. Copyright (2015) American Chemical Society.

Figure S1-6

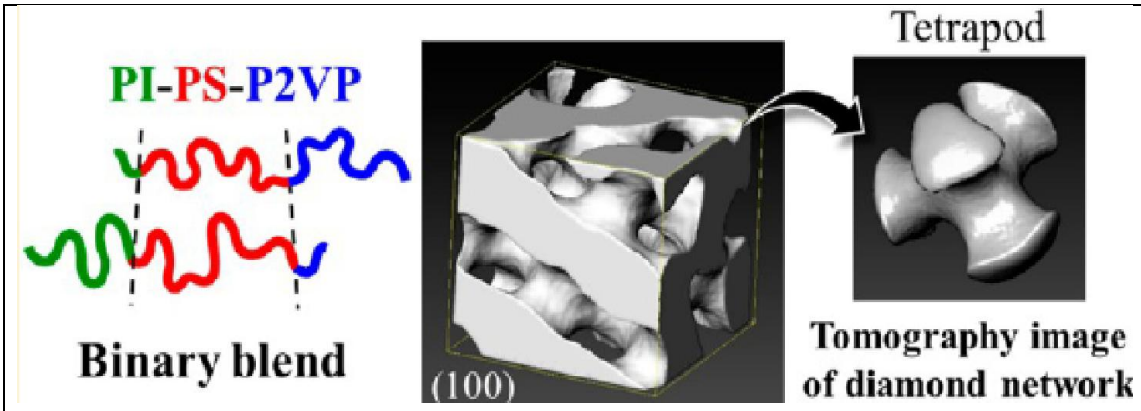

Figure S1-6: 3D TEM tomography reconstructed images for a blend of two asymmetric PI-b-PS-b-P2VP observed by Asai.[22] Reprinted with permission from ref 22. Copyright (2017) American Chemical Society.

Figure S1-7

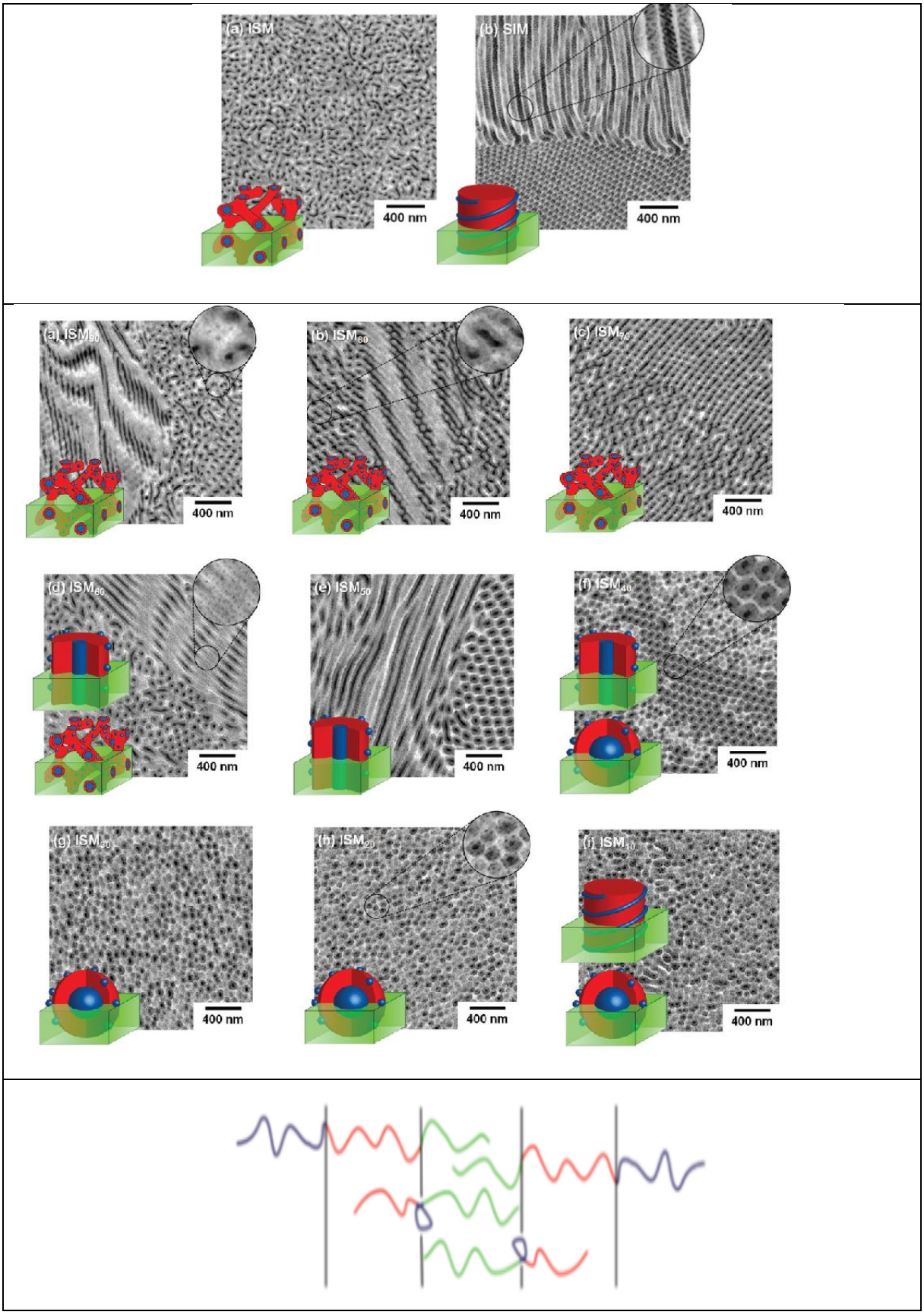
(a) ISM
400 nm
(b) SIM
400 nm
(a) ISM80
400 nm
(b) ISM60
400 nm
(c) ISM40
400 nm
(d) ISM80
400 nm
(e) ISM50
400 nm
(f) ISM40
400 nm
(g) ISM20
400 nm
(h) ISM20
400 nm
(i) ISM10
400 nm

Figure S1-7: TEM images of the morphology observed by Haenelt et al.[24] for a blend of PI-b-PS-b-PMMA and PS-b-PI-b-PMMA and the corresponding schematic illustrations. Reprinted from ref [24] by permission of John Wiley & Sons, Inc. Copyright © 2018 by John Wiley Sons, Inc.

Figure S1-8

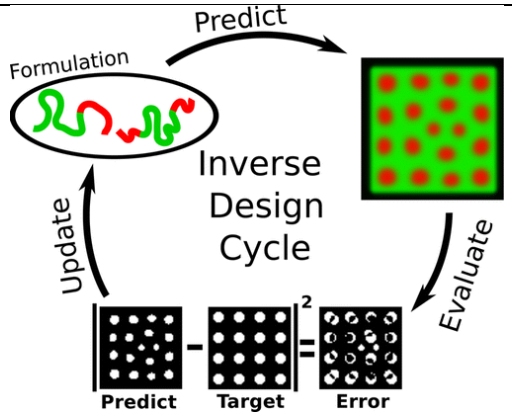

Figure S1-8: Principle of the method proposed by Paradiso et al. [35] for optimizing the block polymer blend to obtain the desired self-assembled polymer pattern. Reprinted with permission from ref [35]. Copyright (2016) American Chemical Society.

Figure S2-1

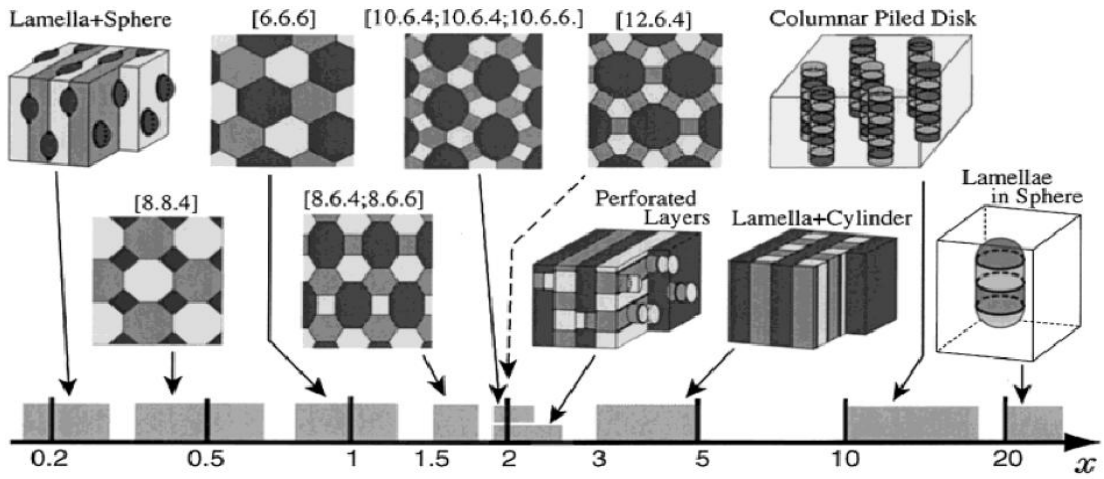

Figure S2-1: Phase diagram of ABC star polymer system with arm-length ratio 1:1:X with symmetric interactions between the three components proposed by Gemma et al.[45] Reprinted with permission from ref [45]. Copyright (2002) American Chemical Society.

Figure S2-2

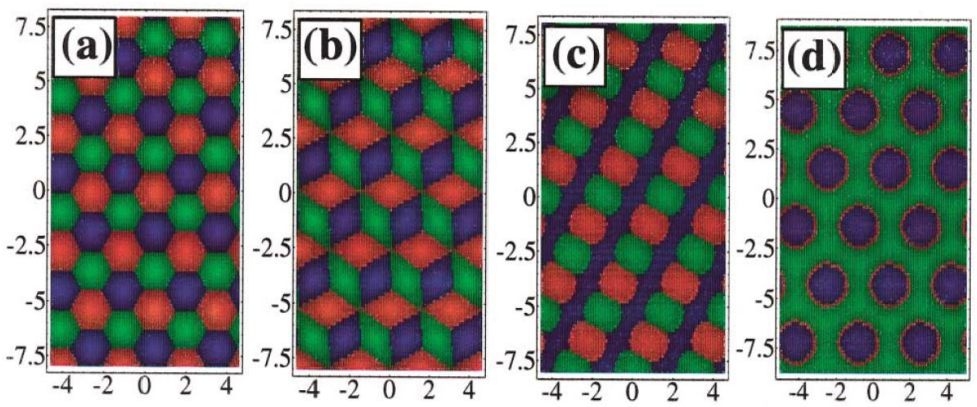

Figure S2-2: Ordered microphases predicted by theoretical calculation based on self-consistent field approach in the work of Bohhot-Aviv and Wang.[47] Reprinted figure with permission from ref [47]. Copyright (2000) by the American Physical Society.

Figure S3-1

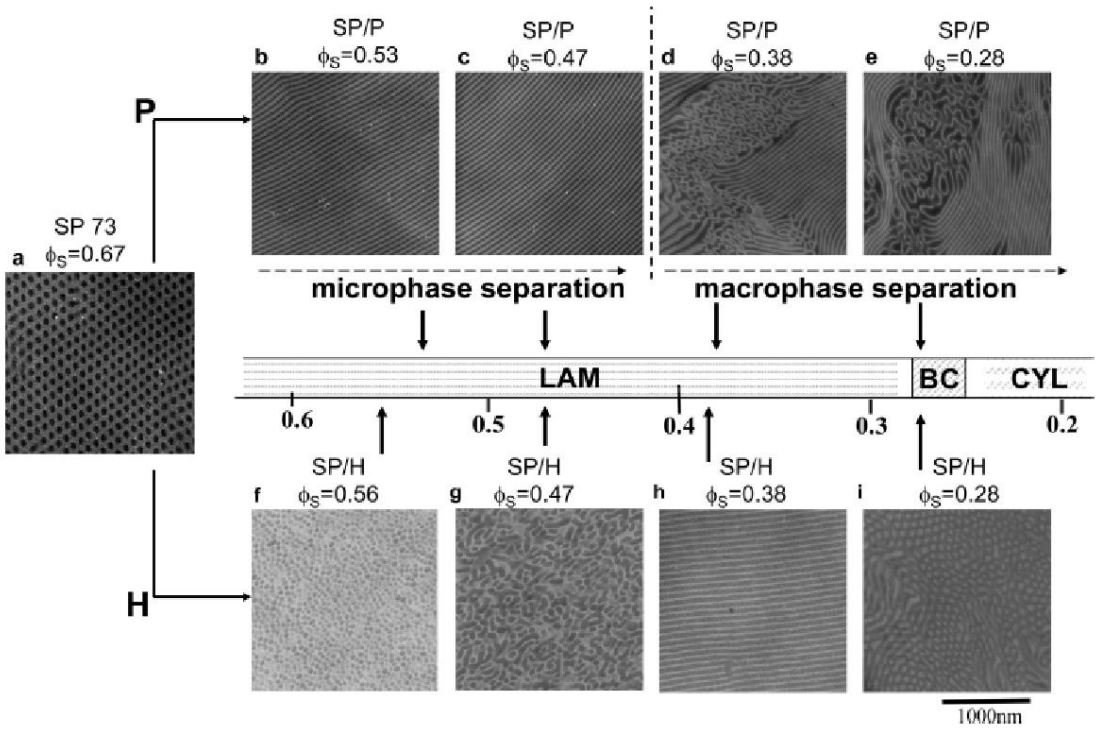

Figure S3-1: TEM images observed by Dobrosielska et al.[63] on blends of SP and P or H. Reprinted with permission from ref [63]. Copyright (2008) American Chemical Society.

Figure 3.2

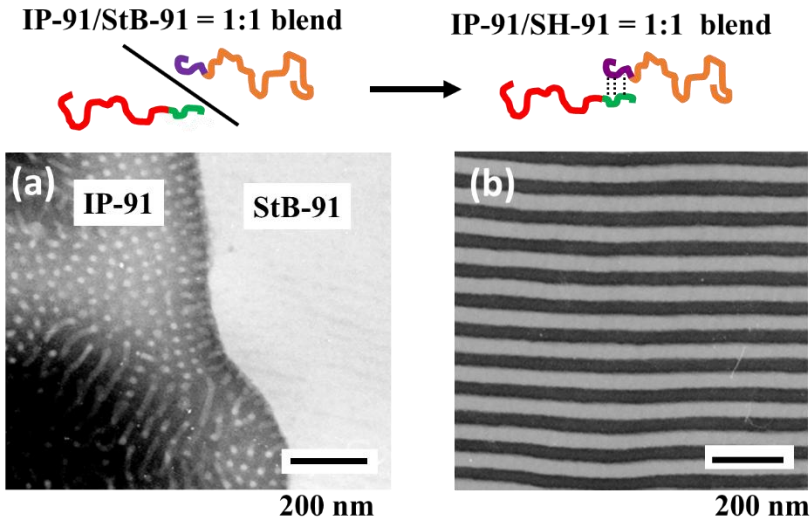

Figure S3-2: TEM images of diblock copolymer blend film stained with OsO_4 for an (a) IP-91/StB-91 1:1, (b) IP-91/SH-91 1:1 in the work of Asari.[66] Reprinted with permission from ref [66]. Copyright (2005) American Chemical Society.

Figure S3-3

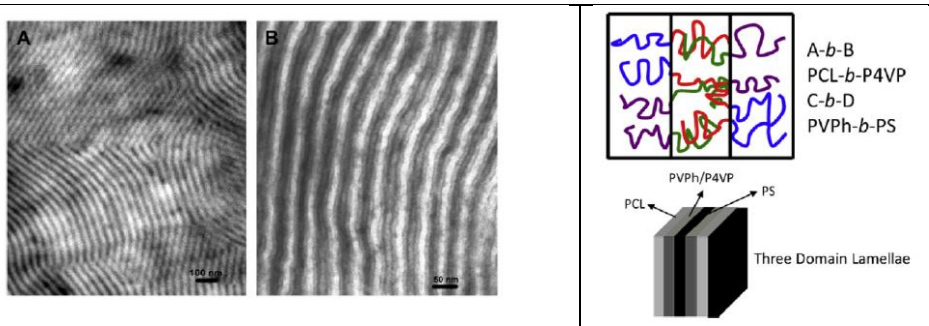

Figure S3-3: TEM images of solution-cast films in the work of Chen et al.[67] of the blend PCL-b-P4VP and PS-b-PVPh 80/20 stained with I_2(A) and RuO_4(B) and the corresponding schematic representation. Reprinted from Ref [67], Copyright (2010), with permission from Elsevier.

Figure S3-4

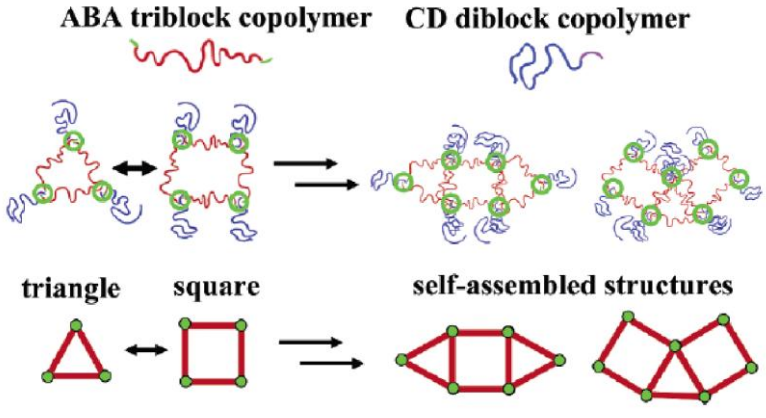

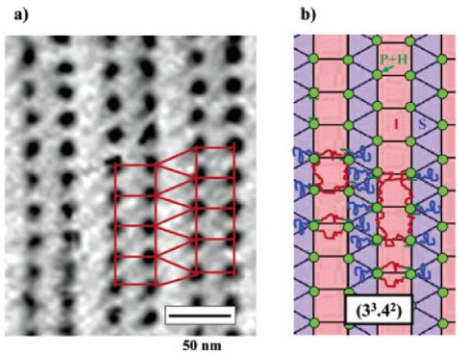

Figure S3-4: Schematic representation of two types of self-assembled "closed-loop" structures and their assembly at the top. (a) A TEM image and (b) the corresponding schematic drawing of a microdomain assembly in the work by Asari[68] for the PIP-91/SH-91 1/1 blend. Reprinted with permission from ref [68]. Copyright (2006) American Chemical Society.

Figure S3-5

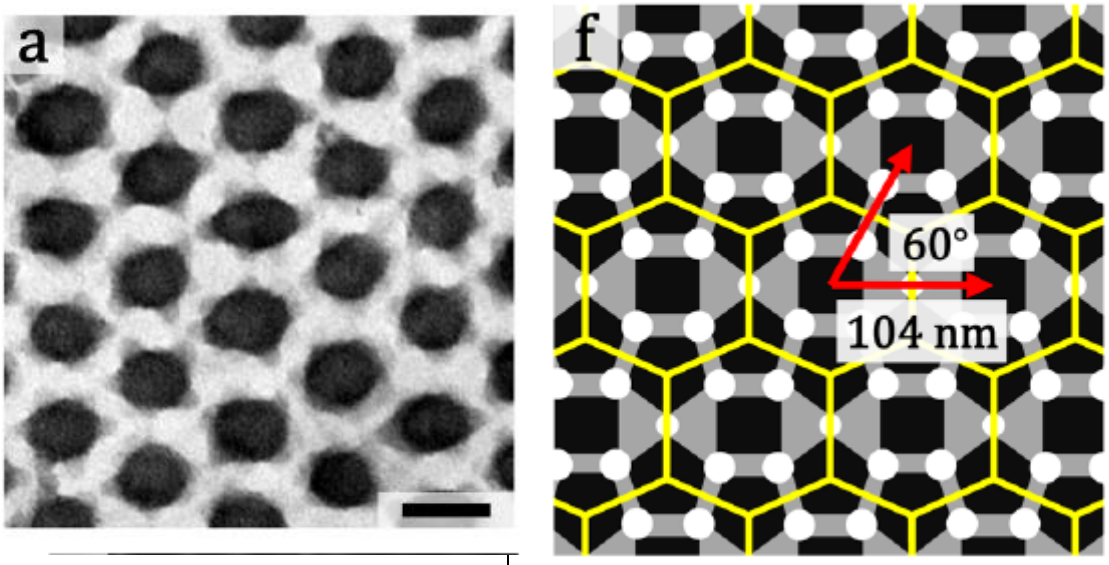

Figure S3-5: (a) A TEM image and (b) the corresponding schematic illustration with yellow lines, which give a unit lattice in Miyase et al.[70] for ISP/HM-0.35 stained with OsO_4/ I_2. Reprinted with permission from ref [70]. Copyright (2017) American Chemical Society.

Table S1. Characteristics parameters of the blends studied in part I

Ref	Polym[1]	Mol. Wt. kg.mol^{-1}	Vol. Fract. f_I:f_S:f_{2VP}	structure parent[2]	block length ratio			blending ratio mol/mol	Polydispersity index			Ave. Com. Vol. Fract. f_I:f_S:f_{2VP}	structure created[2]
					I	S	P		I	S	P		
9	I-S	47.0	0.81:0.19	SPH	4.2	1		0.25/0.75 to 0.59/0.41	1.3 to 1.6	1.0		0.52:0.48 0.68: 0.32	LAM
		18.6	0.51:0.48	LAM	1	1.0		0.69/0.31 to 0.75/0.25	1.2	1.0		0.72:0.28 0.74: 0.26	CYL
		47.0	0.81:0.19	CYL	4.8	1.3		0.21/0.79 to 0.68/0.31	1.2 to 1.8	1.0		0.55:0.45 to 0.73:0.27	LAM
								0.69/0.31 to 0.75/ 0.25	1.2	1.0		0.74:0.26 to 0.75:0.25	BC
		14.5	0.54:0.46	LAM	1	1		0.79/0.21 to 0.95/0.05	1.1	1.0		0.77:0.23 to 0.80:0.20	CYL
		47.0	0.81:0.19	CYL	6.5	1.5		0.2/0.8 to 0.35/0.65	1.8 to 2.1	1.0		0.58: 0.42 to 0.61:0.39	DIS
								0.39/0.61 to 0.78/0.22	1.2 to 1.7	1.0		0.64:0.36 to 0.76:0.24	LAM
		12.1	0.51:0.49	DIS	1	1		0.82/0.18 to 0.84/0.16	1.15	1.0		0.77: 0.23	BC
								0.90/0.10 to 0.97/0.03	1.1	1.0		0.79: 0.21 to 0.81:0.19	CYL
10	I-S	190	0.54:0.46	LAM	3.2	1		0.90/0.1 to 0.80/0.20	1.0 to 1.1	1.0		0.52:0.48 to 0.49: 0.51	LAM
								0.70/0.30 to 0.60/0.40	1.1 to 1.2	1.0		0.46:0.54 to 0.44: 0.56	DG or DD
		124	0.27:0.73	CYL	1	1.0		0.50/0.50 to 0.10/0.90	1.2 to 1.3	1.0		0.41:0.59 to 0.30:0.70	CYL
		190	0.54:0.46	LAM	3.2	1		0.56/0.2/0.24	1.2	1.0		0.55: 0.45	DG

		151 124	0.38:0.62 0.27:0.73	DG CYL	1.7 1	1.1 1.0		0.14/0.8/0.06 0.28/0.6/0.12 0.42/0.4/0.18 0.07/0.90/0.03	1.1 1.0	1.0 1.0		0.43: 0.57 to 0.40:0.60 0.39:0.61	DD DG
11	S-2VP	144 124 115	0.10:0.90 0.50:0.50 0.91:0.09			1 4.5 7.8	11.8 5.8 1	0.2/0.6/0.2 0.33/0.34/0.33		1.2 1.4	1.3 1.5	0.5:0.5 0.5:0.5	LAM LAM
14	I-S-2VP	2.6 9.6 150	0.36:0.34:0.30 0.31:0.39:0.30 0.35:0.33:0.32	LAM LAM LAM	1 3.2 5.6	1 4.2 5.6	1 3.7 6.1	0.15/0.70/0.15 to 0.29/0.43/0.29 to 0.33/0.33/0.33 0.36/0.28/0.36 0.45/0.10/0.45 0.50/0.0/0.50	1.1 to 1.3 1.4 1.5	1.1 to 1.3 1.3 to 1.4 1.5		0.33:0.33:0.33	LAM UL MPS
15	I-S-2VP	122 124	0.06:0.62:0.32 0.39:0.56:0.05	CYL-LAM SPH-LAM	1 7.0	1.0 1	5.9 1	0.50/0.50	1.6	1.0	1.5	0.23:0.59:0.18	ROD
		126 124	0.08:0.52:0.40 0.13:0.55:0.32 0.24:0.55:0.21	SPH-LAM GYR GYR	1 1.6 4.0	1 1.1 1.4	7.6 6.1 5.3	0.20/0.20/0.20/0.20/0.20 0.50/0/0/0/0.50	1.3 1.4	1.0 1.0	1.3 1.6	0.25:0.54:0.21 0.25:0.54:0.21	DG ROD

		161 145 124	0.34:0.55:0.11 0.39:0.56:0.05	GYR SPH-LAM	5.2 5.1	1.3 1.1	2.3 1	0.26/0.17/0.14/0.17/0.26	1.3	1.0	1.4	0.25:0.54:0.21	DG
								0.31/0.15/0.08/0.15/0.31	1.4	1.0	1.4	0.25:0.54:0.21	DG
20	I-S-2VP	122 124	0.06:0.62:0.32 0.39:0.56:0.05	CYL-LAM SPH-GYR	1 7.0	1.0 1	5.9 1	0.60/0.40	1.7	1.0	1.4	0.20:0.60:0.20	ROD
								0.48/0.52	1.5	1.0	1.5	0.24:0.59:0.17	nCMC
								0.40/0.60	1.4	1.0	1.7	0.27:0.58: 0.15	nCMC
21	I-S-2VP	223 264	0.12:0.67:0.21 0.42:0.56:0.02	D-HEX SPH-LAM	1 4.4	1 1.0	8.4 1	0.90/0.10 to 0.40/0.60	1.4 to 1.6	1.0	1.1 to 1.6	0.16:0.66:0.18 to 0.32:0.60:0.08	ROD
								0.30/0.70 to 0.10/0.90	1.1 to 1.3	1.0	1.8 to 2.6	0.34:0.59:0.07 to 0.4:0.57:0.03	MPS
22	I-S-2VP	136 146	0.09:0.42:0.49 0.51:0.40:0.09	p-LAM p-LAM	1 6.6	1 1.1	4.7 1	0.90/0.10	2.2	1.0	1.1	0.13:0.42:0.45	P-LAM
								0.80/0.20	2.1	1.0	1.1	0.18:0.42:0.40	DG
								0.70/0.30 to 0.60/0.40	1.7 to 1.9	1.0	1.2 to 1.3	0.23:0.41:0.36 to 0.27:0.41:0.32	DG+DD
								0.50/0.50 to 0.1/0.9	1.1 to 1.5	1.0	1.4 to 1.6	0.31:0.41:0.24 to 0.47:0.40:0.13	DD

23	I-S-2VP	84	0.12:0.75:0.13	CSC	1	1		0.75/0.25 0.50/0.50	1.0 1.0	1.0 1.0		0.12:0.78:0.10 0.12:0.82:0.07	cs-GYR
	I-S	78	0.11:0.89	SPH	1.0	1.0		0.33/0.67 0.17/0.83	1.0 1.0	1.0 1.0		0.11/0.84/0.04 0.11/0.86/0.02	SPH

1 S/polystyrene, 2-VP/poly2-vinylpyridine, I/polyisoprene

2 LAM/lamella, CYL/cylinder, SPH/sphere, SPH-LAM/sphere in lamella, SPH-GYR/sphere in gyroid, CYL-LAM/cylinder in lamella, D-HEX/double hexagonal cylinder, p-LAM/perforated lamella, ROD/ tetragonal rod , DIS/ Disordered state, BC/bicontinuous, DG/double gyroid, DD/double diamond, UL/undulated lamella, MPS/macrophase separation, nCMC/non-constant-mean-curvature interface, cs-GYR/core-shell gyroid ,CSC/coexisting spheres and cylinders

References

[1] A more accurate description of the location of the block copolymer junction at the interphase would need to consider interfacial thickness, which is given by $(\chi N)^{-1/2}$, where χ and N denote the Flory-Huggins interaction parameter and the degree of polymerization of the whole block copolymer, respectively.

[2] T. Ohta, K. Kawasaki, *Macromolecules* **1986**, *19*, 2621-2632.

[3] N. Hadjichristidis, H. Iatrou, M. Pitsikalis, S. Pispas, A. Avgeropoulos, *Prog. Polym. Sci.* **2005**, *30*,725-78205, see fig 51.

[4] S.H. Han, V. Pryamitsyn, D. Bae, J. Kwak, V. Ganesan, J. K. Kim, *ACS Nano* **2012**, *6*, 7966-7972.

[5] N.A. Lynd, A. J. Meuler, M.A. Hillmyer, *Prog. Polym. Sci.* **2008**, *33*, 875-893.

[6] A. Noro, M. Iinuma, J. Suzuki, A. Takano, Y. Matsushita, *Macromolecules* **2004**, *37*, 3804-3808.

[7] F. Court, T. Hashimoto, *Macromolecules* **2001**, *34*, 2536-2545.

[8] N. Koneripalli, R. Levicky, F. S. Bates, M. W. Matsen, S. K. Satija J. Ankner, H. Kaiser, *Macromolecules* **1998**, *31*, 3498-3508.

[9] F. Court, D.Yamaguchi, T. Hashimoto, *Macromolecules* **2008,** *41*, 4828-4837.

[10] W. Takagi, J. Suzuki, Y. Aoyama, T. Mihira, A. Takano, Y. Matsushita, *Macromolecules* **2019,** *52*, 6633-6640.

[11] A. Noro, M. Okuda, F. Odamaki, D. Kawaguchi, N. Torikai, A. Takano, Y. Matsushita, *Macromolecules* **2006,** *39*, 7654-7661.

[12] Y. Chen, Z. Wang, Y. Gong, H. Huang, T. He, *J. Phys. Chem. B* **2006**, 110, 1647-1655.

[13] R. Guo, H. Huang, Y. Chen, Y.Gong, B. Du, T. He, *Macromolecules* **2008**, *41*, 890-900.

[14] Y. Matsushita, J. Suzuki, Y. Izumi, K. Matsuoka, S.Takahashi, Y. Aoyama, T. Mihira, A. Takano, *J. Chem. Phys.* **2010**, *133*, 194901.

[15] Y. Asai, K. Yamada, M. Yamada, A. Takano, Y. Matsushita, *ACS Macro Letters*, **2014**, 3, 166-169.

[16] A. Guliyeva, M. Vayer, F. Warmont, A.M. Faugère, P. Andreazza, A. Takano, Y. Matsushita, C. Sinturel, , *ACS Macro Lett.* **2018,** *7*, 789-794.

[17] R. Ruiz, E. Dobisz, T.R. Albrecht, *ACS Nano* **2011**, *5*, 79-84.

[18] J.-B. Chang, H. K. Choi, A. F. Hannon, A. Alexander-Katz, C. A. Ross, K. K. Berggren, *Nat. Commun.* **2014**, *5*, 3305.

[19] C. Tang, E. M. Lennon, G. H. Fredrickson, E. J. Kramer, C. J. Hawker, *Science* **2008**, *322*, 429-432.

[20] Y. Asai, A. Takano, Y. Matsushita, *Macromolecules **2015**,48,* 1538-1542.

[21] Y. Asai, A. Takano, Y. Matsushita, *Macromolecules **2016**, 49,* 6940-6946.

[22] Y. Asai, J. Suzuki, Y. Aoyama, H. Nishioka, A. Takano, Y.Matsushita, *Macromolecules* **2017**, *50*,5402-5411.

[23] S. Ahn, J. Kwak, C. Choi, Y. Seo, J. K. Kim, *Macromolecules* **2017**, *50*, 9008-9014.

[24] T. G.Haenelt, C.Abetz, V. Abetz, *Macromol. Chem. Phys.* **2018,** *219*, 1700241.

[25] T. Hashimoto, K.Yamasaki, S. Koizumi, H. Hasegawa, *Macromolecules* **1993**, *26*, 2895-2904.

[26] K. I. Winey, E. L. Thomas, L. J. Fetters, *J. Chem. Phys.* **1991**,*95*, 9367.

[27] M. W. Matsen, *Macromolecules* **1995**, *28*, 5765-5773.

[28] M.S. Tureau, L. Rong, B.S. Hsiao, T. H. Epps, *Macromolecules* **2010**, *43*, 9039-9048.

[29] M. W. Matsen, *J. Chem. Phys.* **1995**,*103*, 3268.

[30] Z.Wu, B. Li, Q.Jin, D. Ding, A.-C. Shi, *J. Phys. Chem. B* **2010,** *114*, 15789-15798.

[31] C. A. Tyler, J. Qin, F.S. Bates, D.C. Morse, *Macromolecules* **2007**, *40*, 4654-4668.

[32] C. M. Bates, F. S. Bates, *Macromolecules* **2017**, *50*, 3-22.

[33] Z. Xu, J.Lin, Q. Zhang, L. Wang , X. Tian, *Polym. Chem.* **2016**, *7*, 3783-3811.

[34] S.-M. Hur, C. J. Garcıa-Cervera, E.J. Kramer, G. H. Fredrickson, *Macromolecules* **2009**, *42*, 5861-5872.

[35] S.P. Paradiso, K. T. Delaney, G. H. Fredrickson, *ACS Macro Lett.* **2016**, *5*, 972-976.

[36] T.Fujimoto, H. Zhang, T. Kazama, Y. Isono, H. Hasegawa, T. Hashimoto, *Polymer***1992**, *33*, 2208-2213.

[37] H. Huckstadt, V. Abetz, R. Stadler, *Macromol. Rapid Commun.* **1996**,*17*, 599-606.

[38] H. Iatrou, N. Hadjichristidis, *Macromolecules* **1992**, *25*, 4649-4651.

[39] N. Hadjichristidis, H. Iatrou et al., *Macromolecules* **1993**, *26*, 5812-5815.

[40] H. Huckstadt, A. Gopfert, R. Stadler, *Macromol. Chem. Phys.* **2000**, *201*, 296-307

[41] K. Yamauchi, K. Takahashi, H. Hasegawa, H. Iatrou, N. Hadjichristidis, T. Kaneko, Y. Nishikawa, H. Jinnai, T. Matsui, H. Nishioka, M. Shimizu, H. Furukawa, *Macromolecules* **2003**, *36*, 6962-6966.

[42] K. Yamauchi, S. Akasaka, H. Hasegawa, H. Iatrou, N. Hadjichristidis, *Macromolecules* **2005**, *38*, 8022-8027.

[43] S. Sioula, N. Hadjichristidis, E. L. Thomas, *Macromolecules* **1998**, *31*, 8429-8432.

[44]T. Dotera, A. Hatano, *J. Chem. Phys.* **1996**, *105*, 8413.

[45] T Gemma, A. Hatano, T. Dotera, *Macromolecules* **2002**, *35*, 3225-3237.

[46] The periodic patterns composed of merely regular polygons whose meeting manner is all the same covering two dimensional space. There are only twelve kinds and they were summarized on p.63 in “Tilings and Patterns” by B. Grunbaum and G.C., Published by W H Freeman & Co (1986). (34.6) tiling has its mirror image.

[47] Y. Bohbot-Raviv, Z.-G. Wang, *Phys. Rev. Lett.* **2000**, *85*, 3428-3431.

[48] P.Tang, F. Qiu, H. Zhang, Y. Yang, *J. Phys. Chem. B* **2004**, *108*, 8434-8438.

[49] J. J. K. Kirkensgaard, *Phys. Rev. E - Stat. Nonlinear, Soft Matter Phys.* **2012**, *85*, 031802.

[50] J. Lequieu, T. Koeper, K. T. Delaney, G. H. Fredrickson, *Macromolecules* **2020**, doi: 10.1021/acs.macromol.9b02254.

[51] Y.-L. Yang, H.-K. Tsao, Y.-J. Sheng, *Macromolecules* **2020**, doi: 10.1021/acs.macromol.9b02621

[52] A. Takano, W. Kawashima, A. Noro, Y. Isono, N. Tanaka, T. Dotera, Y. Matsushita, *J. Polym. Sci. Polym. Part B: Phys. Ed.* **2005,** *43*, 2427-2432.

[53] K. Hayashida, A. Takano, N.Tanaka , Y. Matsushita, , *Macromolecules* **2007**, *40*, 3695-3699.

[54] K. Hayashida, T. Dotera, A. Takano, Y. Matsushita, *Phys. Rev. Lett.* **2007**, *98*, 195502.

[55] K. Aissou, H. K. Choi, A. Nunns, I. Manners, C.A. Ross, *Nano Lett.***2013**, *13*, 835-839.

[56] A. Nunns, C.A. Ross, I. Manners, *Macromolecules* **2013**, *46*, 2628-2635.

[57]Z. Li, M.A. Hillmyer, T.P. Lodge, *Nano Lett.* **2006**, *6*, 1245-1249.

[58] Z. Li, M.A. Hillmyer, T.P. Lodge, *Langmuir* **2006**, *22*, 9409-9417.

[59] J. Ruokolainen, R. Makinen, M. Torkkeli, T. Makela, R. Serimaa, G. ten Brinke, O. Ikkala, *Science* **1998**, *280*, 557.

[60] J. Ruokolainen, M. Saariaho, O. Ikkala, G. ten Brinke, E. L. M. Torkkeli, R. Serimaa, *Macromolecules* **1999**, *32*, 1152-1158.

[61] B. K. Kuila, M. Stamm, *J. Mater. Chem.* **2011**, *21*, 14127.

[62] T. Ruotsalainen, J. Turku, P. Hiekkataipale, U. Vainio, R. Serimaa, G. ten Brinke, A.Harlin, J. Ruokolainen, O. Ikkala, *Soft Matter* **2007**, *3*, 978-985.

[63] K. Dobrosielska, S. Wakao, A. Takano, Y. Matsushita, *Macromolecules* **2008**, *41*,7695-7698.

[64] S. Jiang, A. Göpfert, V. Abetz, *Macromolecules* **2003**, *36*, 6171-6177.

[65] T. Asari, S. Matsuo, A. Takano, Y. Matsushita, *Polym. J* **2006**, *38*, 258-263.

[66] T. Asari, S. Matsuo, A. Takano, Y. Matsushita, *Macromolecules* **2005**, *38*, 8811-8815.

[67] W.C. Chen, S.-W. Kuo, F.-C. Changa, *Polymer* **2010**, *51*, 4176-4184.

[68] T. Asari, S. Arai, A. Takano, Y. Matsushita, *Macromolecules* **2006,** *39*, 2232-2237.

[69] B. D. Mather, M.B. Baker, F. L. Beyer, M. A. G. Berg, M. D. Green, T. E. Long, *Macromolecules* **2017**, *40*, 6834.

[70] H. Miyase, Y. Asai, A. Takano, Y. Matsushita, *Macromolecules* **2017**, *50*, 979-986.